



OPEN Non-targeted metabolomics reveals fatty acid and associated pathways driving resistance to whitefly and tomato leafminer in wild tomato accessions

Sunil Kumaraswamy^{1,2}, Kalenahalli Yogendra³, Paola Sotelo-Cardona^{4,5}, Aparna Shivanna⁶, Sanivarapu Hemalatha³, Muthugounder Mohan¹ & Ramasamy Srinivasan⁴✉

Wild tomato species exhibit natural insect resistance, yet the specific secondary metabolites and underlying mechanisms governing the resistance remain unclear. Moreover, defense expression dynamically adapts to insect herbivory, causing significant metabolic changes and species-specific secondary metabolite accumulation. The present study aims to identify the resistance-related metabolites in wild tomato accessions that influence the defense mechanism against whitefly (*Bemisia tabaci* Asia II 7) and leafminer (*Phthorimaea absoluta*). In this study, LC-HRMS-based non-targeted metabolomics of resistant wild (*Solanum cheesmaniae* and *Solanum galapagense*) and susceptible cultivated (*Solanum lycopersicum*) accessions following 6- and 12-h post-infestation (hpi) by *B. tabaci* Asia II 7 and *P. absoluta* revealed distinct sets of resistance-related constitutive (RRC) and induced (RRI) metabolites. The key resistance-related metabolites were those involved in the fatty acid and associated biosynthesis pathways (e.g., triacontane, di-heptanoic acid, dodecanoic acid, undecanoic acid, N-hexadecanoic acid, pentacosane, monogalactosyldiacylglycerols, sphinganine, and 12-hydroxyjasmonic acid), which are recognized for their direct or indirect role in mediating plant defense against insects. Additionally, the differential accumulation of metabolites was evident through partial least squares-discriminant analysis (PLS-DA), highlighting differences in metabolite profiles between resistant and susceptible accessions at 6 and 12 hpi of *B. tabaci* and *P. absoluta*. Volcano plot analysis revealed a higher number of significantly upregulated metabolites in wild accessions following herbivory. Moreover, wild tomato accessions responded uniquely to *B. tabaci* and *P. absoluta*, highlighting species-specific metabolic responses of tomato accessions to the two feeding guilds. This study uncovered biochemical mechanisms governing resistance in wild tomato accessions, elucidated the influence of dual herbivory on the plant metabolome, and offered well-characterized parent materials and candidate metabolites for breeding insect-resistant varieties.

Keywords Plant–herbivore interaction, Metabolomics, Constitutive and induced metabolites, Whitefly, Tomato leafminer, Plant defense

Tomato, *Solanum lycopersicum* Linnaeus is damaged by two important insect herbivores, the whitefly, *Bemisia tabaci* Gennadius (Hemiptera: Aleyrodidae) and tomato leafminer, *Phthorimaea absoluta* Meyrick (Lepidoptera: Gelechiidae) (Synonym: *Tuta absoluta*). *B. tabaci* causes damage through sap feeding and acts as a disease vector^{1,2}, notably, it exhibits cryptic species complex, including Asia II 7³. At the same time, *P. absoluta* is one of the most destructive pests of tomatoes, resulting in substantial yield losses⁴. Tomatoes are highly susceptible to *B. tabaci* and *P. absoluta* infestations, often necessitating chemical control, resulting in resistance to multiple

¹ICAR-National Bureau of Agricultural Insect Resources, Bengaluru 560024, India. ²Department of Plant Biology, Ecology and Evolution, Oklahoma State University, Stillwater, OK 74078, USA. ³International Crops Research Institute for the Semi-Arid Tropics, Hyderabad 502324, India. ⁴World Vegetable Center, 60 Yi-Min Liao, Shanhua, Tainan 74151, Taiwan. ⁵Oregon IPM Center, Oregon State University, Corvallis, OR 97330, USA. ⁶World Vegetable Center, South and Central Asia, ICRISAT Campus, Hyderabad 502324, India. ✉email: srini.ramasamy@worldveg.org

insecticide classes^{5,6}. Therefore, developing insect-resistant tomatoes is critical to reducing losses from these pests.

Plants have evolved intricate defense systems encompassing physical traits such as thorns, trichomes, and specialized secondary metabolites that deter or harm herbivores⁷. These defenses can be constitutive or induced and emerge as a response to stresses, including herbivory, involving the active synthesis of secondary metabolites⁸. These interacting herbivores induce changes in the plant's metabolome, activating defense metabolites to deter pests⁹. Similarly, in tomatoes resistance to *B. tabaci*^{10,11} and *P. absoluta*^{12,13} is mainly mediated by glandular trichomes and chemical defenses, especially in wild species. Wild tomato species serve as valuable sources of genetic material for breeding resistant cultivars¹⁰. The availability of tomato genotypes and wild tomato species with high resistance levels to *B. tabaci* and *P. absoluta* provides significant potential for developing resistant varieties¹⁴. Additionally, wild accessions of *Solanum galapagense* Darwin & Peralta and *Solanum pimpinellifolium* Linnaeus are closely related to *S. lycopersicum*, providing breeding compatibility¹⁴. However, the biochemical mechanisms underlying tomato resistance, particularly under herbivore stress remain poorly understood. Nonetheless, the metabolomics approach can help unveil the biochemical basis of resistance under herbivore stress.

Previous studies used the metabolomics approach and shown changes in terpenoid and flavonoid profiles in tomatoes in response to *B. tabaci* herbivory^{10,15}, and metabolomics has also been applied to unveil resistance to Tomato yellow leaf curl virus (TYLCV)¹⁶ and Tomato curly stunt virus (ToCSV)¹⁷ transmitted by *B. tabaci*. Similarly, herbivory by *P. absoluta* accumulated phenol amides, spermine dihydro cinnamic acid and induced both phenylpropanoid and polyamine precursor pathways¹⁸ and other compounds, including fatty acids, acylsugars, chlorogenic acid, neochlorogenic acid, and feruloyl quinic acid in tomatoes which govern resistance¹⁹. Additionally, the metabolomics was used to elucidate the biochemical basis of resistance to other tomato pests like western flower thrips, *Frankliniella occidentalis* Pergande²⁰ and spider mites, *Tetranychus urticae* Koch²¹. However, most of these studies relied on a targeted approach, which presented some limitations in the detection range.

Nonetheless, non-targeted metabolomics has proven successful in unraveling the systematic biochemical responses of plants to various stresses²². Liquid chromatography-mass spectrometry (LC-MS) based non-targeted metabolomics can be leveraged to identify endogenous candidate resistance-related (RR) metabolites involved in plant-herbivore interactions and to provide insights into phenotypic variations²³. In plant breeding, metabolomics is a valuable diagnostic tool for evaluating plant performance and investigating essential metabolic markers associated with resistance to biotic or abiotic stress²⁴. Integrating metabolomics with other omics unveils a comprehensive, multi-layered view of systems biology, linking genes to function²⁵. This integration streamlines crop breeding for developing resistant varieties by expanding the genetic pool, identifying novel genes, enabling stress-tolerant introgression breeding, and discovering metabolic traits²⁶.

Host plant resistance proved a highly economical and environmentally friendly long-term pest management strategy. In our previous study, we identified antixenosis and antibiosis basis of resistance in wild tomato accessions of *Solanum cheesmaniae* Riley and *S. galapagense* against *B. tabaci* Asia II 7 and *P. absoluta*¹⁴. However, the specific secondary metabolites and biochemical mechanisms governing insect resistance in these wild tomato species under herbivore stress remain unclear. Understanding these mechanisms is crucial for fully utilizing available genetic resources and advancing knowledge of plant-herbivore interactions to develop novel insect management strategies. Traditionally, plant-herbivore interaction studies focused on the influence of individual herbivory on metabolic changes²⁷. However, plants coexist in complex ecosystems and encounter attacks from multiple insect herbivores, leading to species-specific accumulation of diverse secondary metabolites²⁸. Moreover, herbivore feeding guild and diet breadth may also influence the specificity of induced metabolites, with these metabolites undergoing significant changes over time, potentially reflected in altered metabolic profiles^{29,30}. Since diverse feeding modes influence differential resistance responses, comprehensive studies comparing their effects are lacking.

In the present study, we investigated the biochemical mechanisms of resistance in wild tomato accessions during herbivory by the generalist phloem-feeding *B. tabaci* Asia II 7 and the specialist cryptic leafminer *P. absoluta* at two interaction time points using non-targeted metabolomics. The primary objective was to identify RR metabolites in wild tomato accessions, map candidate metabolites onto critical metabolic pathways and observe species-specific metabolic responses. These findings offer valuable insights for developing insect-resistant varieties and biopesticides, contributing to long-term sustainable pest management strategies.

Results

Differential accumulation of metabolites in wild tomato accessions

LC-HRMS-based non-targeted metabolomics of insect-infested and uninfested tomato accessions at 6 and 12 hpi revealed distinct metabolic responses and uncovered several RR metabolites (Fig. 1). A partial least squares-discriminant analysis (PLS-DA) score plot demonstrated variances in the metabolite profiles between treated (RP and SP) and mock (RM and SM) samples at 6- and 12-h post-infestation (hpi) of *B. tabaci* (Fig. 2) and *P. absoluta* (Fig. 3). In all cases, the metabolite profiles of resistant accessions were clustered together and separated from the susceptible accessions. However, only some overlapping patterns between treated and mock samples of specific accessions were observed, suggesting consistent accumulation of few metabolites. This analysis revealed a noticeable differential accumulation of metabolites across accessions. Additionally, volcano plot analysis of treated and mock samples of each tomato accession revealed significantly upregulated and downregulated metabolites after herbivory at 6 and 12 hpi of *B. tabaci* (Fig. 4) and *P. absoluta* (Fig. 5). In most accessions, the number of metabolites significantly upregulated was higher than those downregulated, especially in resistant wild accessions. This observation indicated a precise response and change in plant metabolome post-herbivory, suggesting a remarkable reprogramming towards metabolite accumulation following herbivory.

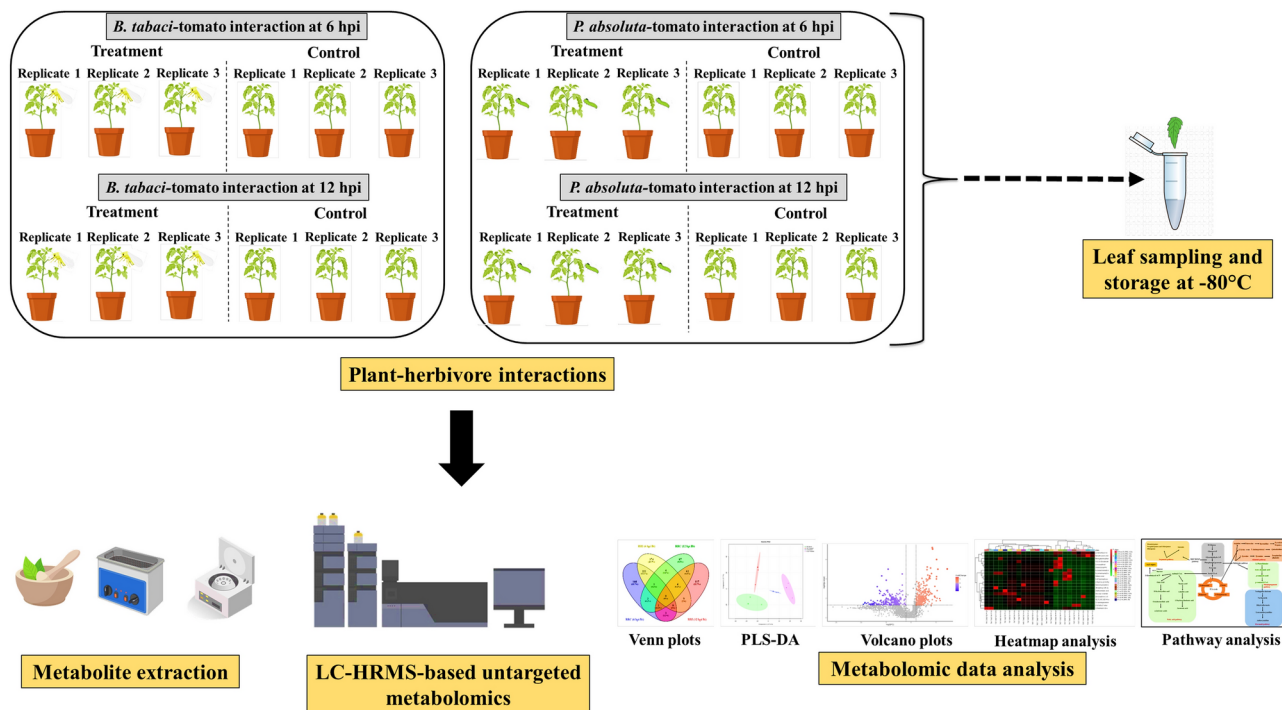


Fig. 1. Overview of metabolomics experimental setup and data analysis for each tomato accession.

Metabolic changes in wild tomato accessions following *B. tabaci* and *P. absoluta* herbivory

Resistance-related constitutive (RRC) metabolites

RRC metabolites with $FC > 1$ were meticulously quantified in resistant (V3, V7 and V10) and susceptible (C5 and H6) tomato accessions in RM_SM comparisons. In *B. tabaci*-tomato interaction at 6 hpi, 7884 consistent peaks of monoisotopic masses were detected with a differential accumulation of 263 constitutive metabolites. This rigorous process ensured the accuracy of our findings. Among RM_SM comparisons, V3 vs. H6 had the highest number of constitutive metabolites, whereas V7 vs. H6 had the lowest (Table S1). At 12 hpi of *B. tabaci*, 4786 consistent peaks of monoisotopic masses were detected with a differential accumulation of 161 constitutive metabolites. V3 vs. H6 recorded the highest number of constitutive metabolites, whereas V10 vs. C5 had the lowest (Table S2). In *P. absoluta*-tomato interaction, at 6 hpi, 2851 consistent peaks of monoisotopic masses were detected with differential accumulation of 135 constitutive metabolites. The most constitutive metabolites were observed in V3 vs. C5, while V7 vs. H6 had the lowest (Table S3). At 12 hpi of *P. absoluta*, 2284 consistent peaks of monoisotopic masses were detected with a differential accumulation of 155 constitutive metabolites in RM_SM comparisons. V3 vs. H6 exhibited the highest number of constitutive metabolites, while V7 vs. C5 had the lowest (Table S4).

Resistance-related induced (RRI) metabolites

RRI metabolites with $FC > 1$ were quantified in resistant and susceptible tomato accessions in RP_SP comparisons. In *B. tabaci*-tomato interaction at 6 hpi, a differential accumulation of 503 induced metabolites was found. Among RP_SP comparisons, V7 vs. H6 exhibited the highest number of induced metabolites, whereas V10 vs. C5 had the lowest (Table S5). At 12 hpi of *B. tabaci*, a differential accumulation of 195 induced metabolites was found. The highest number of induced metabolites was found in V3 vs. H6, while V7 vs. C5 had the lowest (Table S6). In *P. absoluta*-tomato interaction at 6 hpi, a differential accumulation of 197 induced metabolites was found. The highest number of induced metabolites was found in V3 vs. H6 whereas V7 vs. C5 had the lowest (Table S7). At 12 hpi of *P. absoluta*, a differential accumulation of 162 induced metabolites was found in RP_SP comparisons. The highest number of induced metabolites was found in V3 vs. H6, while V7 vs. C5 had the lowest (Table S8).

Wild tomato accessions responded uniquely to *B. tabaci* and *P. absoluta* herbivory

Venn diagrams were generated to compare unique and shared constitutive and induced metabolites in *B. tabaci* and *P. absoluta*-tomato interactions. At 6 hpi of *B. tabaci*, 144(15.7%) unique RRC and 374(40.7%) unique RRI metabolites were found, with 111(12.1%) shared metabolites between RRC and RRI groups. At 12 hpi of *B. tabaci*, 87(9.5%) unique RRC, 117(12.7%) unique RRI, and 61(6.6%) shared metabolites were found. Notably, *B. tabaci* herbivory induced the highest number of unique RRI metabolites, with few shared metabolites between 6 and 12 hpi (Fig. 6A). At 6 hpi of *P. absoluta*, 67(14%) unique RRC and 130(27.1%) unique RRI metabolites were found, with 54(11.3%) shared metabolites between RRC and RRI groups. *P. absoluta* herbivory induced the highest number of unique RRI metabolites at 6 hpi. At 12 hpi of *P. absoluta*, 64(13.4%) unique RRC and

A Partial least squares-discriminant analysis (PLS-DA) at 6 hpi of *B. tabaci*

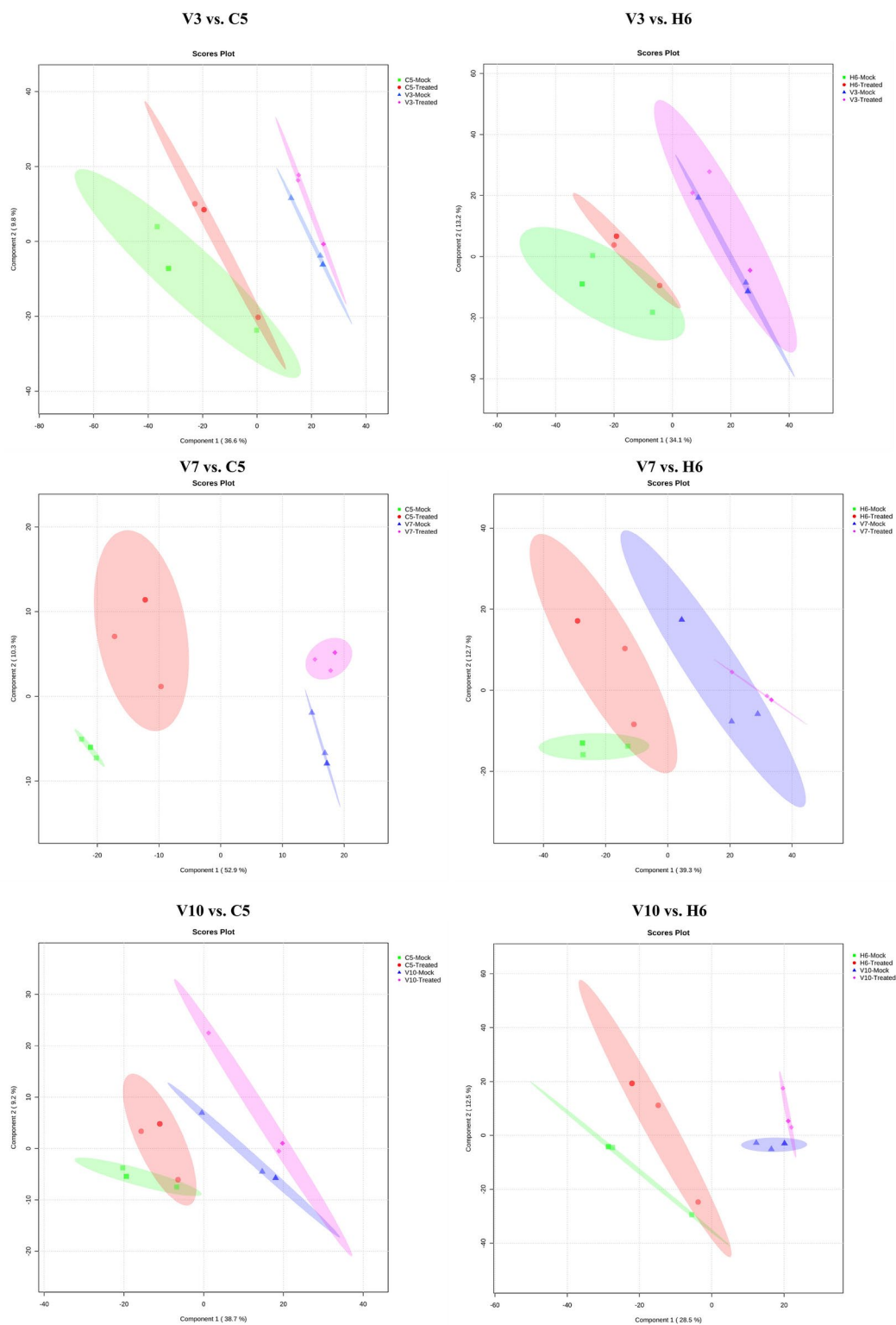


Fig. 2. PLS-DA of metabolic profiles of treated and mock samples of resistant vs. susceptible accessions at (A) 6 hpi of *B. tabaci* and (B) 12 hpi of *B. tabaci*.

B Partial least squares-discriminant analysis (PLS-DA) at 12 hpi of *B. tabaci*

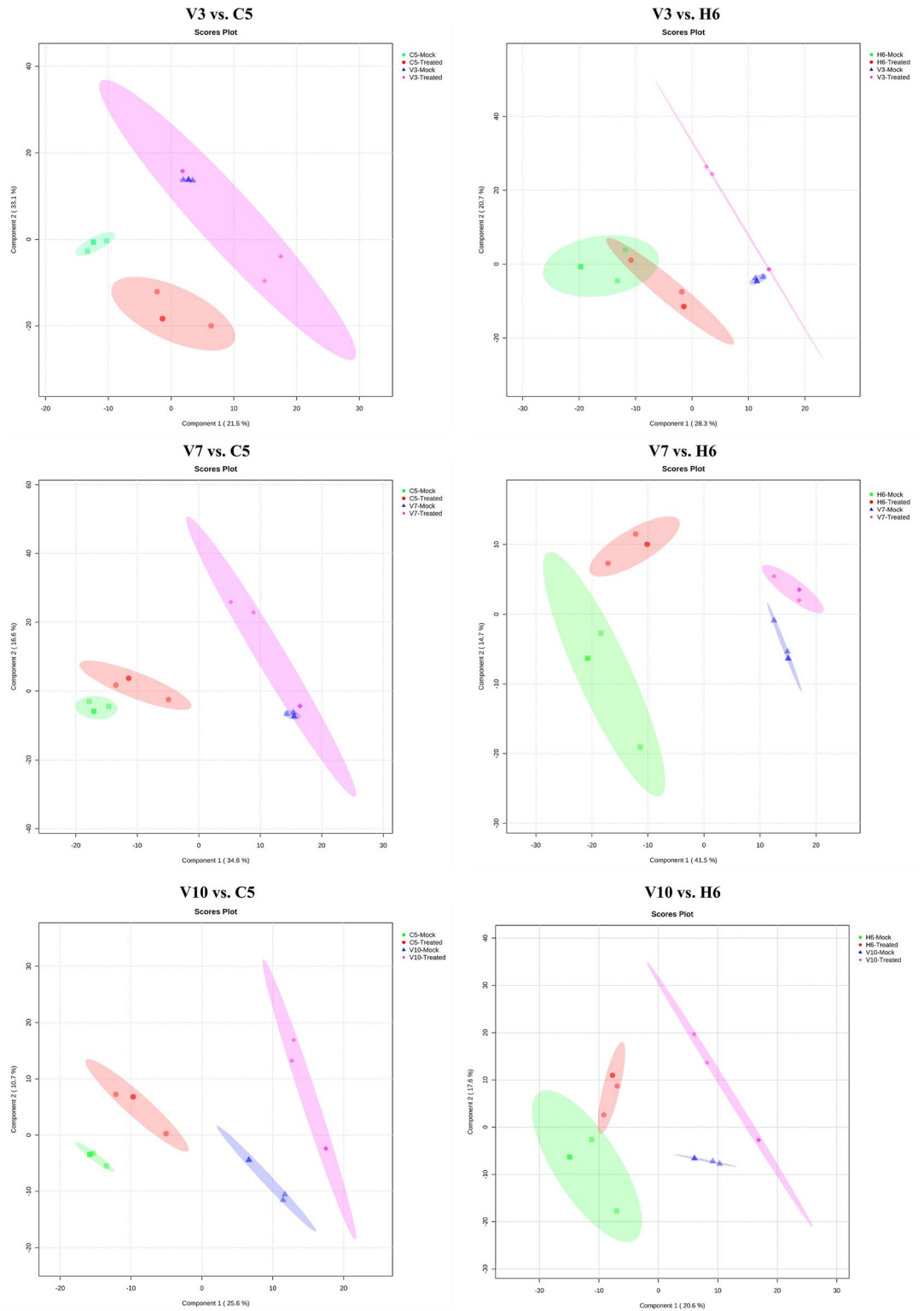


Figure 2. (continued)

66(13.8%) unique RRI metabolites were found, with 80(16.7%) shared metabolites suggesting some consistency in metabolite accumulation before and after *P. absoluta* herbivory. Nevertheless, between 6 and 12 hpi, only a few shared metabolites were found (Fig. 6B). Furthermore, the Venn diagram analysis of metabolites detected in two insect interactions revealed 871(64.5%) unique metabolites in the *B. tabaci*-tomato interaction, 431(31.9%)

A Partial least squares-discriminant analysis (PLS-DA) at 6 hpi of *P. absoluta*

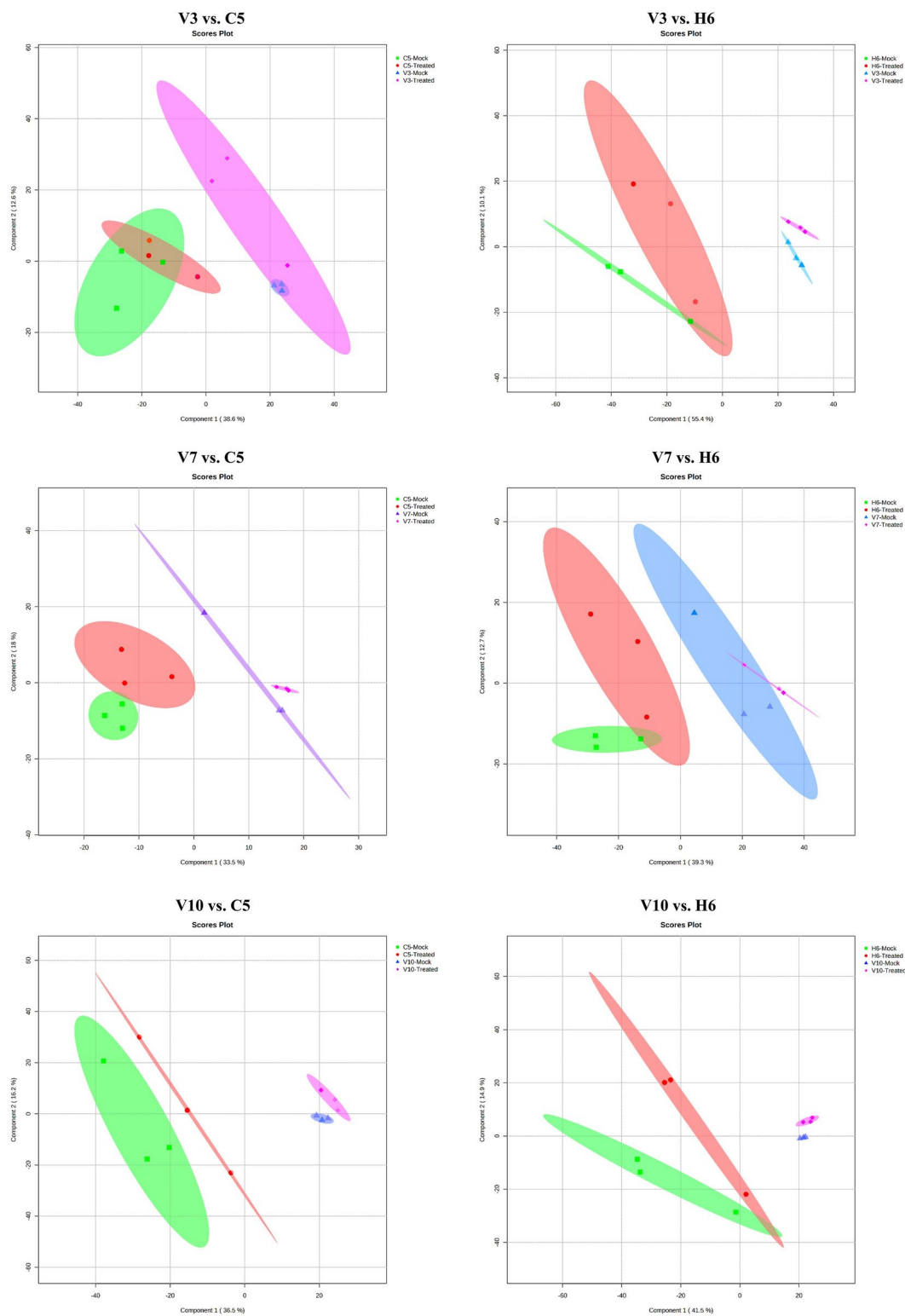


Fig. 3. PLS-DA of metabolic profiles of treated and mock samples of resistant vs. susceptible accessions at **(A)** 6hpi of *P. absoluta* and **(B)** 12 hpi of *P. absoluta*.

B Partial least squares-discriminant analysis (PLS-DA) at 12 hpi of *P. absoluta*

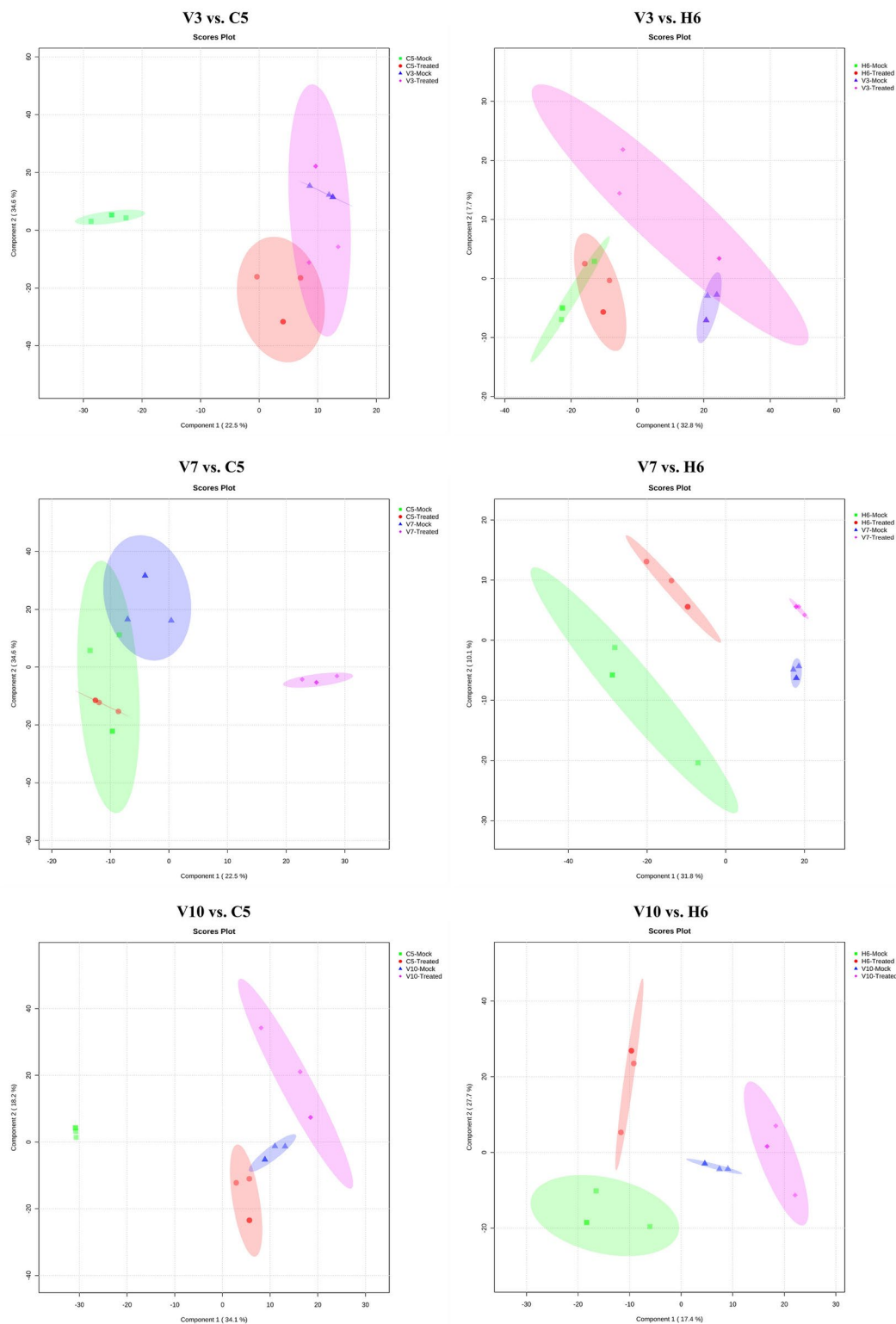


Figure 3. (continued)

unique metabolites in the *P. absoluta*-tomato interaction, and only 48(3.6%) shared metabolites between two insects. This highlights the distinct metabolic responses of wild tomato accessions to insects belonging to two feeding guilds (Fig. 7).

A

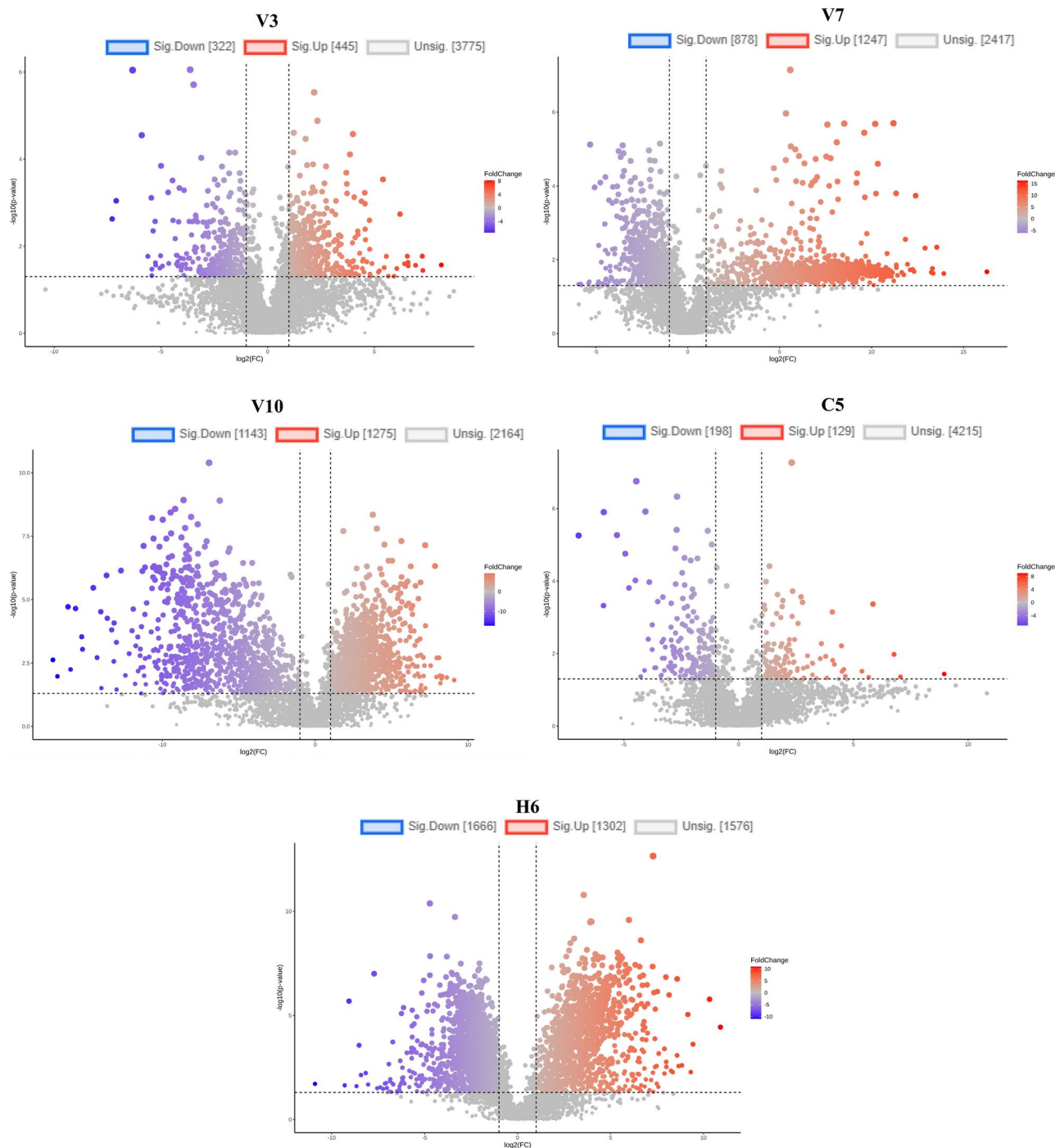
Volcano plots at 6 hpi of *B. tabaci*

Fig. 4. Volcano plots of treated and mock samples of tomato accessions depicting metabolites that were significantly (p -value < 0.05) changed in accumulation at (A) 6 hpi of *B. tabaci* and (B) 12 hpi of *B. tabaci*.

Metabolites related to plant defense

Various chemical groups of RR metabolites, including fatty acids, flavonoids, terpenoids, alkaloids, amino acids, and phenylpropanoids, were identified (Tables S1 to S8). The fatty acid and associated biosynthesis pathways were the key resistance-governing pathways in *B. tabaci* and *P. absoluta*-tomato interaction (Tables 1 and 2). These RR metabolites in fatty acid and associated biosynthesis pathways belong to different classes such as fatty acids, jasmonic acids, glycerolipids, glycerophospholipids, sphingolipids and acylsugars and induce direct effects, repellent, and/or feeding deterrent action against insects (Fig. 8). These RR metabolites were also involved in

B

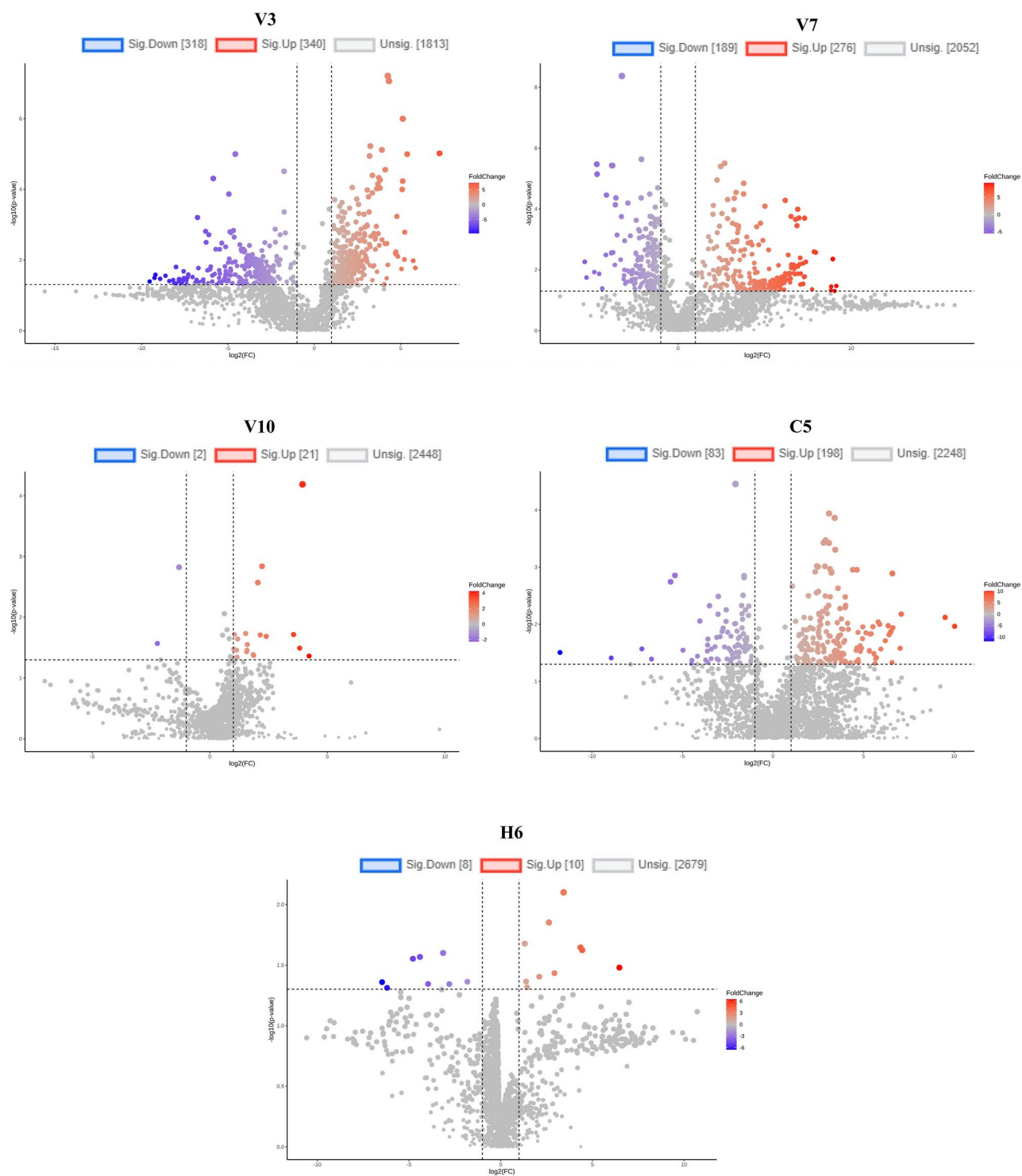
Volcano plots at 12 hpi of *B. tabaci*

Figure 4. (continued)

plant–insect interactions, tri-trophic interactions, and plant defense signaling. The differential accumulation of these RR fatty acid and associated pathway metabolites with variable FC values across resistant vs. susceptible comparisons at 6 and 12 hpi of *B. tabaci* and *P. absoluta* are visualized in hierarchical clustering with the heat maps (Fig. 9).

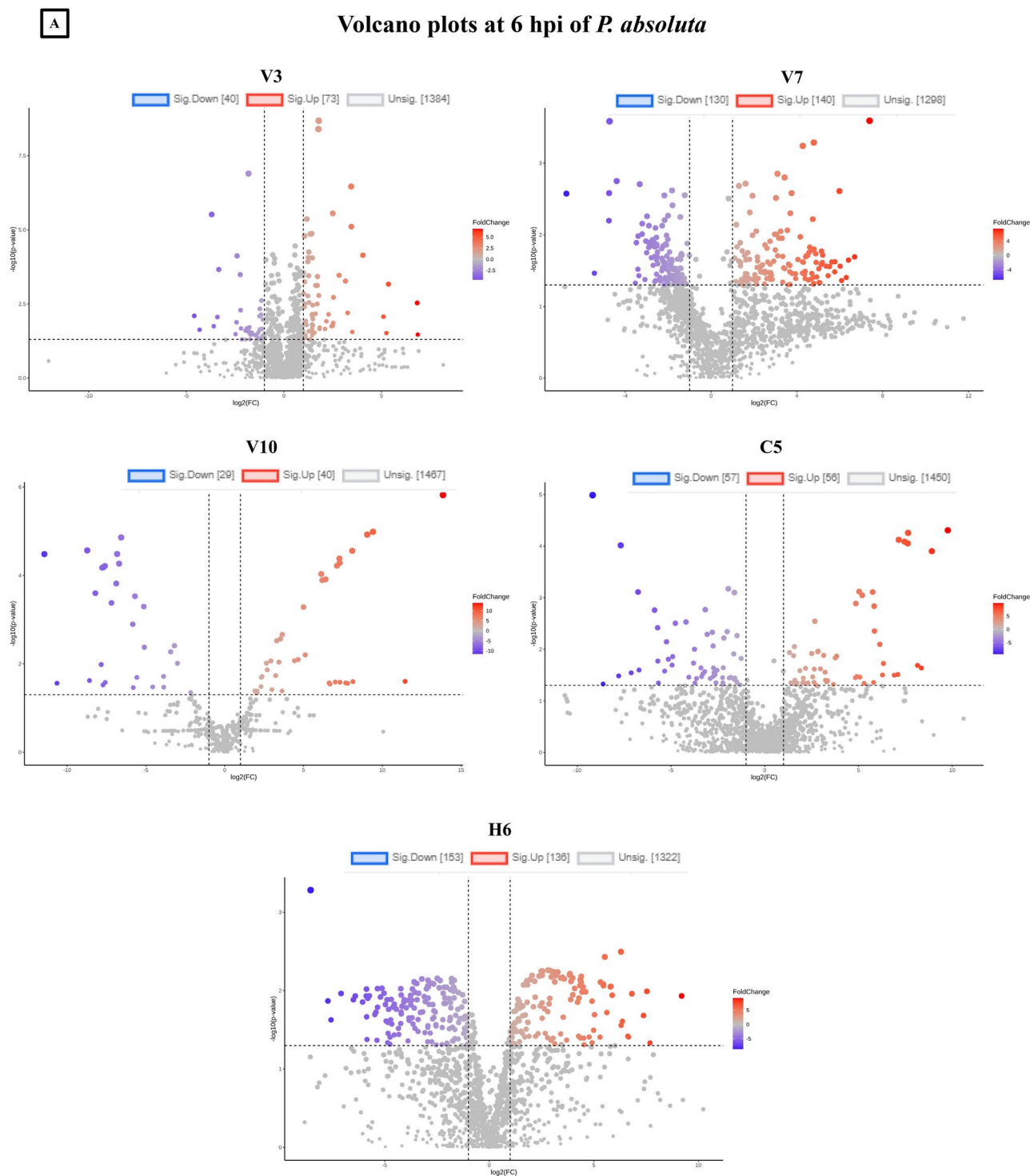


Fig. 5. Volcano plots of treated and mock samples of tomato accessions depicting metabolites that were significantly (p value < 0.05) changed in accumulation at (A) 6 hpi of *P. absoluta* and (B) 12 hpi of *P. absoluta*.

Discussion

Plant–herbivore interactions have shaped complex plant defense systems³¹. Non-targeted metabolomics plays a crucial role in uncovering these defenses by providing detailed and comprehensive metabolic profiling²². Considering the differential plant responses induced by herbivores of different feeding guilds, holistic studies examining their impact on metabolomes are limited. Some studies, including those on tomatoes, have noted distinct responses of plants to herbivory from different feeding guilds. For instance, single and multiple infestations by *T. urticae* and green peach aphids, *Myzus persicae* Sulzer induced a specific biochemical response³². Similarly, the generalist herbivore, *Helicoverpa zea* Boddie altered more metabolites than the specialist, *Manduca*

B

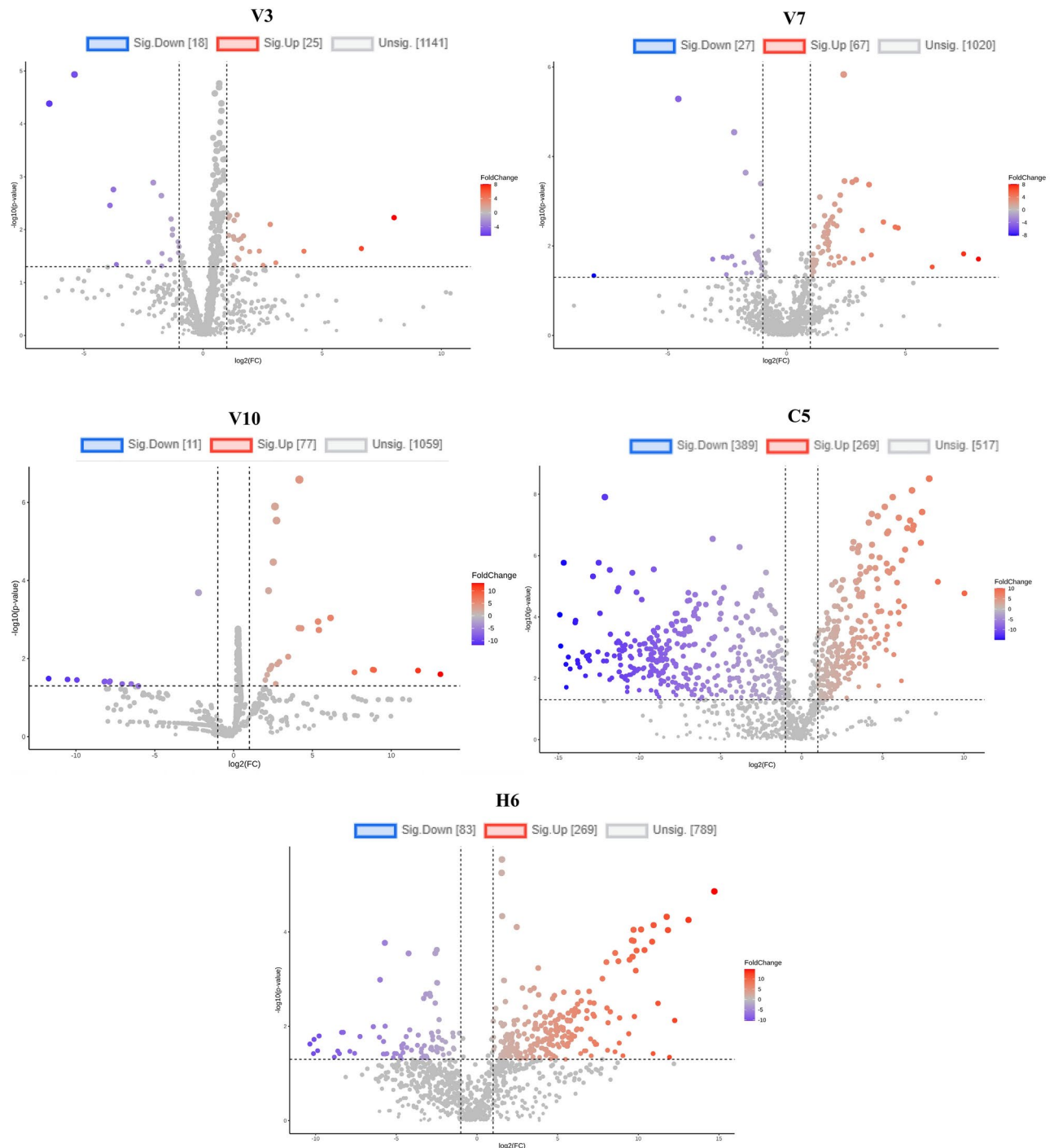
Volcano plots at 12 hpi of *P. absoluta*

Figure 5. (continued)

*sexta*³³. Additionally, Beet armyworm, *Spodoptera exigua* Hübner induced increased proteinase inhibitor activity, contrasting with the unaffected activity during potato aphid, *Macrosiphum euphorbiae* Thomas feeding^{34,35}.

Similarly, differential plant responses to herbivory from different feeding guilds have been documented in potato³⁶, tobacco³⁷, cabbage³⁸, cotton³⁹, Brassica⁴⁰, and *Arabidopsis thaliana* Linnaeus⁴¹. We observed differential and insect-specific accumulation of metabolites in resistant wild tomato accessions, V7, V3, and V10 at 6 and 12 hpi of *B. tabaci* Asia II 7 and *P. absoluta* indicating the specific chemical signatures (defense response) of wild tomato accessions. These findings align with previous studies highlighting the temporal dynamics of induced plant responses, as seen in the metabolic profiles of other crops. For instance, elevated phytohormone levels were

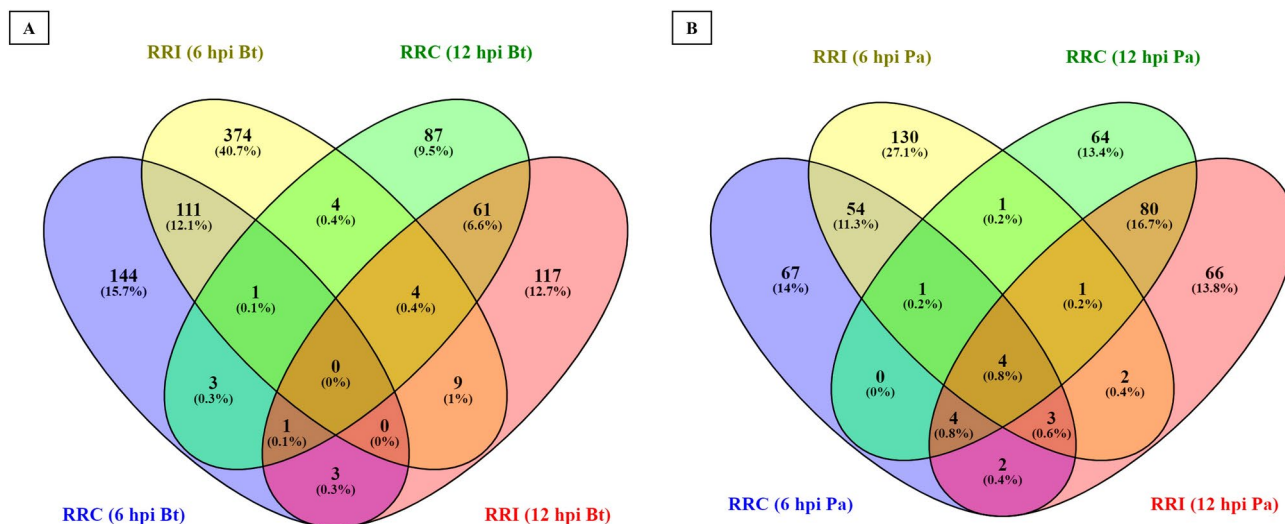


Fig. 6. Venn diagram depicting unique and shared RRC and RRI metabolites. (A) Between 6 and 12 hpi Bt (hours post infestation of *B. tabaci*). (B) Between 6 and 12 hpi Pa (hours post infestation of *P. absoluta*).

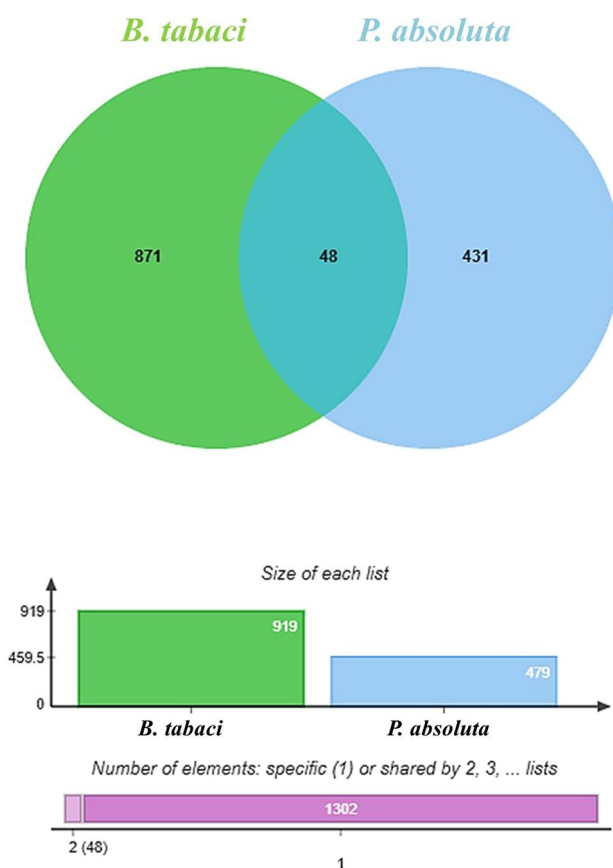


Fig. 7. Venn depicting unique and shared metabolites between *B. tabaci* and *P. absoluta*-tomato interaction.

observed in sorghum at 1, 3, and 6 dpi following *Melanaphis sacchari* Zehntner infestation⁴². Similarly, brown plant hopper, *Nilaparvata lugens* Stål infestation in rice induced metabolic alterations in phenylpropanoid, flavonoid, and terpenoid pathways, leading to increased levels of schaftoside and iso-schaftoside after 24 hours⁴³. Similarly, metabolomics of *N. lugens*-infested rice varieties revealed elevated lipid metabolism pathways at various time points⁴⁴.

| Observed mass | Exact mass | Metabolite name | Pathway group | Fold change | | | | | | Cumulative fold change |
|-----------------|------------|---|---------------|------------------|------------------|------------------------------------|-----------------------------------|------------------|------------------|------------------------|
| | | | | V3 vs. C5 | V3 vs. H6 | V7 vs. C5 | V7 vs. H6 | V10 vs. C5 | V10 vs. H6 | |
| (a) Fatty acids | | | | | | | | | | |
| 314.2454 | 314.2457 | (9Z)-(7S,8S)-Dihydroxy octadecenoic acid | Fatty acids | 4.13 (RRC, 12 h) | 4.48 (RRC, 12 h) | 5.19 (RRC, 12 h) | 5.63 (RRC, 12 h) | – | 1.59 (RRI, 12 h) | 21.02 |
| 344.256 | 344.2563 | 12,13-dihydroxy-11-methoxy-9-octadecenoic acid | Fatty acids | – | – | – | – | 3.83 (RRC, 6 h) | – | 3.83 |
| 397.2821 | 397.2828 | 11 β -PGF ₂ α -ethanolamine | Fatty acids | – | – | – | – | 1.79 (RRI, 12 h) | – | 1.79 |
| 590.6733 | 590.673 | 13,17,21-Trimethylnona triacontane | Fatty acids | – | – | – | – | 1.70 (RRI, 12 h) | – | 1.70 |
| 380.3302 | 380.329 | 15-oxo-18Z-tetracosenoic acid | Fatty acids | 1.13 (RRI, 12 h) | 1.36 (RRI, 6 h) | 2.61 (RRI, 12 h) | 9.44 (RRI, 6 h); 1.60 (RRI, 12 h) | 1.28 (RRI, 12 h) | – | 17.42 |
| 368.3675 | 368.3654 | Tetracosanoic acid | Fatty acids | – | – | – | – | 1.22 (RRI, 6 h) | – | 1.22 |
| 414.3695 | 414.3709 | Tetracosanoic acid 15,16-dihydroxy methyl ester | Fatty acids | – | – | – | 1.28 (RRI, 6 h) | – | – | 1.28 |
| 374.1791 | 374.1802 | 16-dimethylarsinoyl-9Z-hexadecenoic acid | Fatty acids | 1.1 (RRI, 6 h) | 2.76 (RRI, 6 h) | 1.24 (RRI, 6 h) | 3.1 (RRI, 6 h) | – | – | 8.20 |
| 292.2222 | 292.2214 | 2,2-difluoro-hexadecanoic acid | Fatty acids | – | – | 1.25 (RRI, 6 h) | 42.42 (RRI, 6 h) | – | – | 43.67 |
| 382.1372 | 382.1369 | 2-iodo-hexadecanoic acid | Fatty acids | – | – | – | 5.03 (RRI, 6 h) | – | – | 5.03 |
| 330.2935 | 330.2934 | Eicosanoic acid | Fatty acids | 1.70 (RRC, 12 h) | 1.48 (RRC, 12 h) | 13.85 (RRC, 12 h) | 12.06 (RRC, 12 h) | – | – | 29.09 |
| 304.2248 | 304.225 | 2,15,16-trihydroxy palmitic acid | Fatty acids | 2.06 (RRI, 12 h) | 1.05 (RRI, 12 h) | 1.91 (RRI, 12 h) | – | 2.48 (RRI, 12 h) | 1.27 (RRI, 12 h) | 8.77 |
| 564.5813 | 564.5845 | 2,4,6,8-tetramethyl-tetracontanoic acid | Fatty acids | – | 4.48 (RRC, 12 h) | – | – | – | – | 4.48 |
| 820.7844 | 820.7884 | 2-docosyl-3-hydroxy-30-carboxy-triacontanoic acid | Fatty acids | – | – | – | 1.84 (RRC, 12 h) | 5.69 (RRI, 12 h) | – | 7.53 |
| 848.8223 | 848.8197 | 2-eicosyl-3-hydroxy-34-carboxy-tetracontanoic acid | Fatty acids | 2.02 (RRC, 12 h) | 2.62 (RRC, 12 h) | 4.31 (RRC, 12 h); 1.12 (RRI, 12 h) | 5.59 (RRC, 12 h) | – | – | 15.66 |
| 218.2032 | 218.2035 | 2,6,10-Trimethyl-(E,E)-2,6,10,12-tridecatetraene | Fatty acids | – | – | – | 1.39 (RRI, 6 h) | – | – | 1.39 |
| 142.1356 | 142.1358 | 2,6-Dimethyl-5-heptanol | Fatty acids | – | – | 2.42 (RRC, 6 h) | 2.67 (RRC, 6 h) | – | – | 5.09 |
| 204.1115 | 204.111 | N-(3-carboxypropanoyl)-N-hydroxy putrescine | Fatty acids | – | 13.45 (RRI, 6 h) | – | – | – | – | 13.45 |
| 342.2773 | 342.277 | 3-Acetoxy stearic acid | Fatty acids | 5.37 (RRC, 6 h) | – | – | 1.31 (RRI, 6 h) | – | – | 6.68 |
| 326.2471 | 326.2457 | 8-methoxy-13-hydroxy-9,11-octadecadienoic acid | Fatty acids | 1.67 (RRI, 6 h) | 1.45 (RRI, 6 h) | – | – | – | – | 3.12 |
| 312.2898 | 312.2904 | Arachidonic acid | Fatty acids | 1.13 (RRI, 6 h) | – | – | – | – | – | 1.13 |
| Continued | | | | | | | | | | |

| Observed mass | Exact mass | Metabolite name | Pathway group | Fold change | | | | | | Cumulative fold change |
|--------------------------|------------|---|----------------------|--|--|--|-----------------------------------|------------------|-----------------------------------|------------------------|
| | | | | V3 vs. C5 | V3 vs. H6 | V7 vs. C5 | V7 vs. H6 | V10 vs. C5 | V10 vs. H6 | |
| 584.5554 | 584.5532 | Gondoyl-linolenate | Fatty acids | – | – | 24.21 (RRC, 12 h) | 44.16 (RRC, 12 h) | – | – | 68.37 |
| 396.4316 | 396.4331 | Heptacosanol | Fatty acids | 1.60 (RRC, 12 h) | 3.15 (RRI, 12 h) | – | 2.16 (RRI, 12 h) | – | 4.84 (RRI, 12 h) | 11.75 |
| 526.451 | 526.4498 | Lignoceryl serotonin | Fatty acids | – | – | – | 1.34 (RRI, 12 h) | – | 1.30 (RRI, 12 h) | 2.64 |
| 440.3418 | 440.3403 | Oleoyl Serotonin | Fatty acids | – | – | – | – | 1.62 (RRC, 6 h) | 2.33 (RRC, 6 h) | 3.95 |
| 414.3261 | 414.3246 | Palmitoyl Serotonin | Fatty acids | 1.33 (RRI, 6 h) | 1.55 (RRI, 6 h) | – | – | – | – | 2.88 |
| 540.463 | 540.4655 | Pentacosanyl serotonin | Fatty acids | 1.78 (RRI, 6 h) | 14.06 (RRI, 6 h) | 1.0 (RRI, 6 h) | – | 2.97 (RRI, 6 h) | – | 19.81 |
| 284.2647 | 284.2653 | Linoleic acid | Fatty acids | – | – | 3.29 (RRI, 6 h) | – | – | – | 3.29 |
| 352.4066 | 352.4069 | Pentacosane | Fatty acids | – | 1.11 (RRI, 6 h) | – | – | – | – | 1.11 |
| 164.1205 | 164.1201 | cis-Jasmone | Jasmonic acids | – | – | – | 2.15 (RRI, 12 h) | – | – | 2.15 |
| (b) Glycerolipids | | | | | | | | | | |
| 802.4893 | 802.4867 | Linolipin B | Glycerolipids | – | 1.51 (RRC, 6 h) | – | – | – | – | 1.51 |
| 762.4923 | 762.4918 | Linolipin G | Glycerolipids | – | 1.05 (RRI, 12 h) | 2.35 (RRI, 6 h) | 3.39 (RRI, 6 h) | – | – | 6.79 |
| 798.5325 | 798.5282 | Monogalactosyldiacylglycerol | Glycerolipids | 9.01 (RRC, 6 h); 2.64 (RRI, 12 h); 1.78 (RRI, 6 h) | 1.95 (RRC, 12 h); 4.95 (RRI, 12 h); 3.24 (RRI, 6 h); 2.94 (RRC, 6 h) | 1.37 (RRI, 12 h); 2.31 (RRI, 6 h); 2.44 (RRI, 6 h) | 2.58 (RRI, 12 h); 5.01 (RRI, 6 h) | – | 1.20 (RRI, 12 h); 1.49 (RRC, 6 h) | 42.91 |
| 672.3372 | 672.3357 | Digalactosylmonoacylglycerol | Glycerolipids | – | – | – | – | 1.05 (RRI, 12 h) | 1.01 (RRI, 12 h) | 2.06 |
| (c) Glycerophospholipids | | | | | | | | | | |
| 760.5973 | 760.5982 | Docosanoic acid | Glycerophospholipids | – | – | 1.65 (RRI, 6 h) | 3.17 (RRI, 6 h) | – | 1.45 (RRI, 6 h) | 6.27 |
| 672.4704 | 672.473 | 9,12-Octadecadienoic acid | Glycerophospholipids | – | 1.29 (RRI, 6 h) | – | – | – | – | 1.27 |
| (d) Sphingolipids | | | | | | | | | | |
| 397.2593 | 397.2593 | Phytosphingosine 1-phosphate | Sphingolipids | 3.89 (RRC, 6 h); 1.07 (RRI, 6 h) | 46.61 (RRC, 6 h) | – | – | 4.09 (RRC, 6 h) | 48.95 (RRC, 6 h) | 104.61 |
| 303.276 | 303.2773 | Phytosphingosine | Sphingolipids | – | – | – | – | – | 6.23 (RRI, 6 h) | 6.23 |
| 821.7799 | 821.7836 | N-(34-hydroxy-tetracontanoyl)-hydroxyceramide | Ceramides | 1.94 (RRI, 6 h) | 2.77 (RRC, 12 h); 1.94 (RRI, 6 h) | 2.25 (RRC, 12 h) | 25.13 (RRC, 12 h) | 6.91 (RRI, 12 h) | 2.52 (RRI, 6 h); 1.59 (RRI, 12 h) | 45.05 |
| Continued | | | | | | | | | | |

| Observed mass | Exact mass | Metabolite name | Pathway group | Fold change | | | | | | Cumulative fold change |
|----------------|------------|---|---------------|--|-------------------|---|-------------------|--------------------------------------|------------------|------------------------|
| | | | | V3 vs. C5 | V3 vs. H6 | V7 vs. C5 | V7 vs. H6 | V10 vs. C5 | V10 vs. H6 | |
| 713.5442 | 713.5442 | Glucosylceramides (GlcCers) | Ceramides | 1.93 (RRI, 6 h); 2.06 (RRI, 6 h) | 11.11 (RRI, 6 h) | 1.45 (RRI, 6 h); 1.01 (RRI, 12 h) | 32.55 (RRI, 6 h) | 4.42 (RRI, 6 h); 1.59 (RRI, 12 h) | 99.45 (RRI, 6 h) | 155.57 |
| 637.6395 | 637.6373 | N-(tricosanoyl)-sphinganine | Ceramides | 39.18 (RRC, 12 h); 1.28 (RRI, 12 h) | 27.21 (RRC, 12 h) | 122.31 (RRC, 12 h); 4.23 (RRI, 12 h) | 84.95 (RRC, 12 h) | 2.22 (RRI, 12 h) | 1.24 (RRI, 12 h) | 282.62 |
| 779.7731 | 779.7731 | N-(dotriacontanoyl)-phytoceramide | Ceramides | – | 5.05 (RRC, 12 h) | – | – | – | – | 5.05 |
| (e) Acylsugars | | | | | | | | | | |
| 362.231 | 362.2305 | 3R-hydroxy-11R-(3,6-dideoxy- α -L-arabino-hexopyranosyloxy)-dodecanoic acid | Fatty acids | 17.03 (RRC, 12 h) | 14.70 (RRC, 12 h) | – | 4.92 (RRC, 12 h) | 1.31 (RRI, 12 h) | 1.41 (RRI, 12 h) | 39.37 |
| 417.1806 | 417.1788 | 6R-((1H-indol-3-ylcarbonyl)3,6-dideoxy- α -L-arabino-hexopyranosyloxy)-2E-heptenoic acid | Fatty acids | 18.34 (RRC, 6 h) | 6.23 (RRC, 6 h) | – | 2.91 (RRI, 6 h) | 14.85 (RRC, 6 h) | 5.04 (RRC, 6 h) | 47.37 |

Table 1. Resistance-related fatty acid and associated pathway metabolites in *B. tabaci*-tomato interaction involved in plant defense against insects, observed at 6 and 12 hpi. *RRC* resistance-related constitutive, *RRI* resistance-related induced, *6h* 6 h post infestation, *12h* 12 h post infestation.

Fatty acid metabolites are major structural and metabolic constituents of the cell wall, involved in fatty acid biosynthesis, elongation, and degradation. We observed differential accumulation of fatty acid and associated pathway metabolites in wild accessions. Only a few previous studies have reported the role of different metabolites in governing resistance to *B. tabaci* and *P. absoluta* in tomatoes. For example, acylsugars have been shown to play a key role in whitefly defense, with whitefly-resistant tomatoes exhibiting elevated concentrations of these compounds in their glandular trichomes¹⁰. Similarly, whitefly-resistant *S. galapagense* displayed higher acylsugar levels⁴⁵. Infestation by *B. tabaci* altered terpenoid and flavonoid profiles¹⁵, with increased flavonoid production deterring *B. tabaci* landing and settling in tomatoes⁴⁶. Moreover, flavonoid accumulation not only enhanced direct defenses but also induced volatile organic compounds (VOCs) in response to *B. tabaci* feeding⁴⁷. Furthermore, metabolic reprogramming of various metabolites was observed in resistant *S. lycopersicum* lines following whitefly-mediated ToCSV infection¹⁷. Resistance to *P. absoluta* is similarly associated with the accumulation of various metabolites. Herbivory by *P. absoluta* stimulates the production of fatty acids, acyl sugars, chlorogenic acid, and feruloyl quinic acid in tomato plants¹⁹. Furthermore, damage by *P. absoluta* activates the phenylpropanoid and polyamine precursor pathways in tomato plants¹⁸. The infestation also triggers the accumulation of secondary metabolites and VOCs, including aldehydes, alcohols, alkanes, phenols, and terpenes⁴⁸, all of which may contribute to the plant's defense response. The fatty acid and associated pathway metabolites identified in our study suggest their involvement in defense mechanisms, including insecticidal action, plant–insect interactions, tri-trophic interactions, and defense signaling processes.

Fatty acids related to insect repellent, deterrent and insecticidal action

Previous reports have shown that 2,4-nonadienal and propionic acid demonstrated repellent and harmful effects against wheat weevil, *Sitophilus granarius* Linnaeus and rice weevil, *Sitophilus oryzae* Linnaeus^{49,50}. Undecanoic acid exhibited vigorous antifeedant activity against *M. persicae* and *B. tabaci*⁵¹. Similarly, 9,12-octadecadienoic acid, and 9,12,15-octadecatrienoic acid methyl ester demonstrated strong insecticidal activity against *A. gossypii*⁵². Additionally, 9-octadecenoic acid and tetradecanoic acid exhibited oviposition deterrent and larvicidal effects on cotton bollworm, *Helicoverpa armigera* Hübner⁵³. Furthermore, 1-palmitoyl-2-linoleoyl-3-glycerophosphocholine effectively controlled cotton aphids, *Aphis gossypii* Glover on cucumber⁵⁴, and in resistant wheat plants, 1-palmitoyl-glycerophosphocholine was mobilized into fatty acids, conferring resistance against the Hessian fly, *Mayetiola destructor* Say⁵⁵.

The glossy-leaved cabbage genotype (NY 8329) containing 14-heptacosanol reduced the preference by diamondback moth, *Plutella xylostella* Linnaeus larvae⁵⁶. Similarly, stearic acid induced antibiosis resistance against spotted stem borer, *Chilo partellus* Swinhoe⁵⁷, and integration of silver nanoparticles with stearic acid demonstrated oviposition deterrent and ovicidal activity against spotted bollworm, *Earias vittella* Fabricius⁵⁸. Likewise, triacontane, identified in *P. absoluta*-resistant tomato accessions⁵⁹, inhibited fall armyworm, *Spodoptera frugiperda* Smith, yellow mealworm, *Tenebrio molitor* Linnaeus, and fruit fly, *Drosophila melanogaster* Meigen⁶⁰. The acylsugar compound dodecanoic acid, identified as an acyl constituent of 3',3,4,6-tetra-O-acyl sucroses complex in glandular trichomes of *S. pennellii* and wild potato, *Solanum berthaultii* Hawkes which exhibited repellent activity against *M. euphorbiae* and *M. persicae*^{61–63}. Similarly, di-heptanoic acid and acylsucroses, induced mortality of *M. persicae* and *B. tabaci*^{64,65}.

| Observed mass | Exact mass | Metabolite name | Pathway group | Fold change | | | | | | Cumulative fold change |
|--------------------------|------------|---|----------------------|-------------------|-------------------------------------|-------------------|-------------------------------------|-------------------|-------------------|------------------------|
| | | | | V3 vs. C5 | V3 vs. H6 | V7 vs. C5 | V7 vs. H6 | V10 vs. C5 | V10 vs. H6 | |
| (a) Fatty acids | | | | | | | | | | |
| 138.1043 | 138.1045 | 2,4-nonadienal | Fatty acids | - | 101.44 (RRC, 12 h) | - | 241.69 (RRC, 12 h) | - | - | 343.13 |
| 144.0784 | 144.0786 | 3-butyrl propionic acid | Fatty acids | - | 16.34 (RRC, 12 h) | - | 19.12 (RRC, 12 h) | - | - | 35.46 |
| 202.1215 | 202.1205 | Sebacic acid | Fatty acids | - | - | - | - | 12.03 (RRC, 6 h) | 65.76 (RRC, 6 h) | 77.79 |
| 216.1374 | 216.1362 | Undecanedioic acid | Fatty acids | - | - | - | 1.36 (RRI, 6 h) | - | - | 1.36 |
| 248.1772 | 248.1776 | 4Z,7Z,10Z,13Z-hexadecatetraenoic acid | Fatty acids | 9.12 (RRI, 12 h) | - | - | - | - | - | 9.12 |
| 268.276 | 268.2766 | 9Z-Octadecen-1-ol | Fatty acids | - | - | - | - | - | 6.82 (RRI, 12 h) | 6.82 |
| 338.3169 | 338.3185 | 2,4-dimethyl-2-eicosenoic acid | Fatty acids | 52.01 (RRI, 12 h) | 38.45 (RRC, 12 h); 2.39 (RRI, 12 h) | 27.24 (RRI, 12 h) | 42.36 (RRC, 12 h); 1.25 (RRI, 12 h) | 22.62 (RRI, 12 h) | 39.79 (RRI, 12 h) | 226.11 |
| 376.2474 | 376.2461 | 3R-hydroxy-12R-(3,6-dideoxy- α -L-arabino-hexopyranosyloxy)-tridecanoic acid | Fatty acids | - | - | - | - | 1.03 (RRI, 6 h) | - | 1.03 |
| 398.3779 | 398.376 | 2-Hydroxy-22-methyltetracosanoic acid | Fatty acids | - | 4.44 (RRC, 12 h) | - | - | - | - | 4.44 |
| 688.3339 | 688.334 | 2-O-Sulfo-2'-stearoyl- α , α -trehalose | Fatty acids | - | - | 1.93 (RRI, 12 h) | 1.90 (RRI, 12 h) | - | - | 3.83 |
| 386.1939 | 386.1941 | 12-hydroxyjasmonic acid 12-O-beta-D-glucoside | Jasmonic acids | - | - | 2.14 (RRC, 6 h) | - | - | - | 2.14 |
| (b) Glycerolipid | | | | | | | | | | |
| 726.5251 | 726.5282 | Monogalactosyldiacylglycerol | Glycerolipid | - | - | - | 4.71 (RRC, 12 h) | - | 1.14 (RRI, 6 h) | 5.85 |
| (c) Glycerophospholipids | | | | | | | | | | |
| 692.4388 | 692.4417 | 9,12,15-Octadecatrienoic acid | Glycerophospholipids | 19.34 (RRI, 12 h) | 55.74 (RRC, 12 h) | - | 67.42 (RRC, 12 h) | - | - | 142.5 |
| 593.3718 | 593.3693 | 1-Palmitoyl-2-(5-oxovaleroyl)-sn-glycero-3-phosphorylcholine | Glycerophospholipids | 56.68 (RRC, 6 h) | 51.38 (RRC, 6 h) | - | - | 3.19 (RRC, 6 h) | 2.89 (RRC, 6 h) | 114.14 |
| 694.4751 | 694.4785 | Hexadecanoic acid | Glycerophospholipids | - | 1.95 (RRC, 12 h); 2.78 (RRI, 12 h) | - | 1.67 (RRI, 12 h) | 78.28 (RRI, 12 h) | 4.64 (RRI, 12 h) | 89.32 |
| (d) Sphingolipids | | | | | | | | | | |
| 937.6936 | 937.6983 | N-(hexacosanoyl)-4R-hydroxysphinganine-1-phospho-(1'-myo-inositol) | Sphingolipids | - | - | - | 2.79 (RRC, 6 h) | - | 3.01 (RRC, 6 h) | 5.8 |
| Continued | | | | | | | | | | |

| Observed mass | Exact mass | Metabolite name | Pathway group | Fold change | | | | | | Cumulative fold change |
|---------------|------------|--|---------------|------------------|------------------|-----------|------------------|----------------------------------|----------------------------------|------------------------|
| | | | | V3 vs. C5 | V3 vs. H6 | V7 vs. C5 | V7 vs. H6 | V10 vs. C5 | V10 vs. H6 | |
| 667.6086 | 667.6115 | N-(2-hydroxytricosanoyl)-hydroxyceramide | Ceramides | - | - | - | - | 276.55 (RRC, 6 h) | 262.56 (RRC, 6 h) | 539.11 |
| 697.546 | 697.5493 | Glucosyl ceramide | Ceramides | 11.33 (RRI, 6 h) | 16.79 (RRI, 6 h) | - | 14.65 (RRI, 6 h) | 7.54 (RRI, 6 h) | 11.18 (RRI, 6 h) | 61.49 |
| 721.7344 | 721.7312 | N-(nonacosanoyl)-sphinganine | Ceramides | - | - | - | - | 7.97 (RRC, 6 h); 4.43 (RRI, 6 h) | 5.87 (RRC, 6 h); 5.18 (RRI, 6 h) | 23.45 |

Table 2. Resistance-related fatty acid and associated pathway metabolites in *P. absoluta*-tomato interaction involved in plant defense against insects, observed at 6 and 12 hpi. RRC resistance-related constitutive, RRI resistance-related induced, 6h 6 h post infestation, 12h 12 h post infestation.

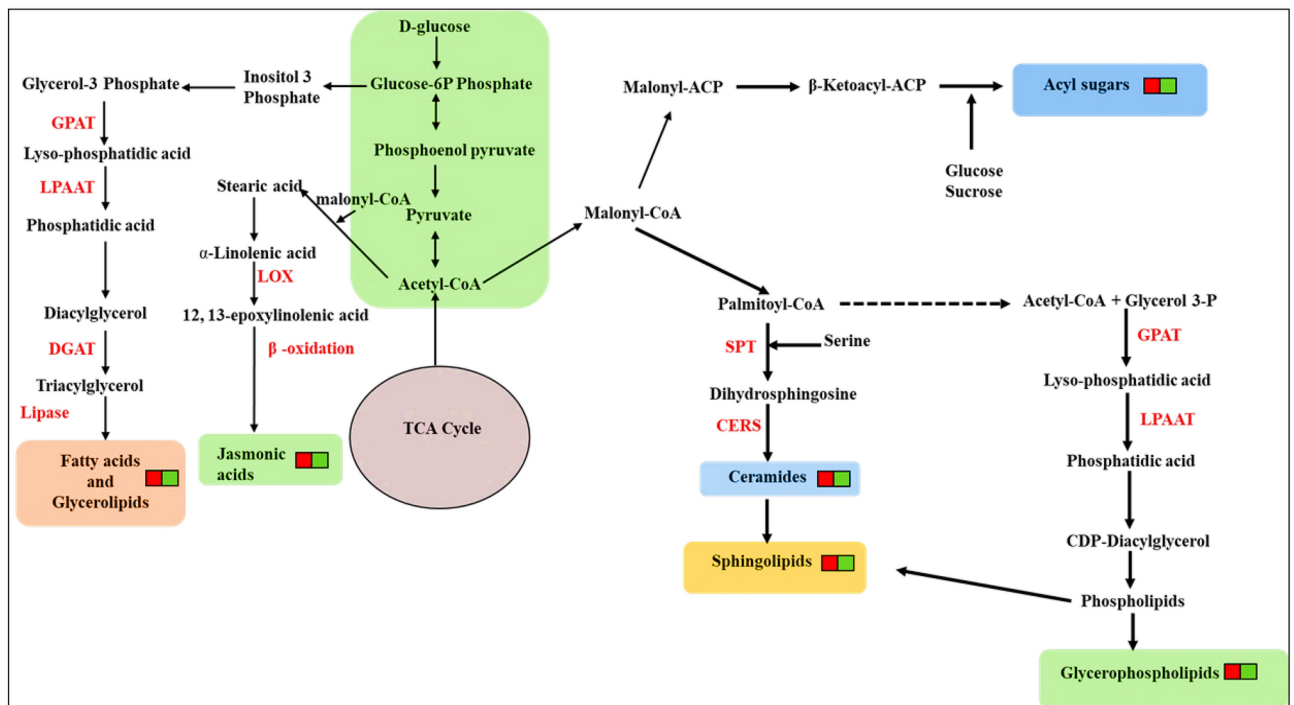


Fig. 8. Fatty acid and associated biosynthesis pathways involved in *B. tabaci* and *P. absoluta*-tomato interactions. This red and green color code indicate that the metabolite groups expressed in both *B. tabaci* and *P. absoluta*-tomato interactions.

Cis-jasmone demonstrated efficacy in repelling wheat grain aphid, *Sitobion avenae* Fabricius⁶⁶, negatively impacting the settling and performance of *M. euphorbiae* on primed potato plants⁶⁷ and promoting higher parasitism levels on *H. armigera* larvae by *Camponotus chlorideae* Uchida on treated tobacco plants⁶⁸. Cis-jasmone was used as a foliar spray to inhibit stink bugs, *Euschistus heros* Fabricius on soybean⁶⁹ and *M. persicae* on Chinese cabbage⁷⁰. At the same time, (*Z*)-jasmone exhibited repellent effects against lettuce aphids, *Nasonovia ribisnigri* Mosley and reduced damson-hop aphids, *Phorodon humuli* Schrank and cereal aphids in wheat plots⁷¹. Similarly, arachidonic acid-producing transgenic *A. thaliana* resisted *M. persicae* by inducing elevated levels of jasmonic acid and stress-responsive genes⁷². It also demonstrated potential as a foliar protectant against Colorado potato beetle, *Leptinotarsa decemlineata* Say⁷³.

Fatty acids related to plant–insect and tri-trophic interactions

Volatile compound, (E, E)-4,8,12-trimethyl-1,3,7,11-tridecatetraene was accumulated as herbivore-induced volatile in plants (tomato, broad bean, French bean, cotton, cucumber, apple, lima bean, corn, and tobacco)^{48,74–76}. Similarly, using portable electronic nose systems, herbivore-induced volatile, N-hexadecanoic acid was used to

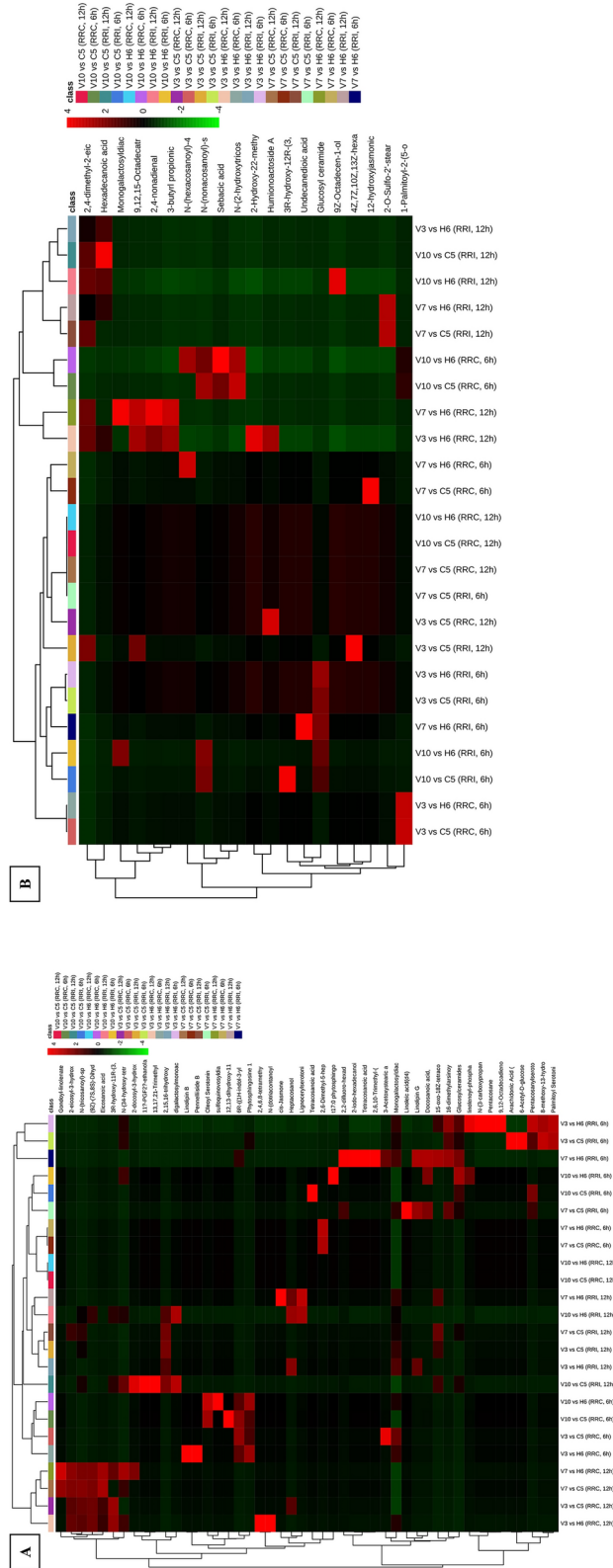


Fig. 9. A hierarchical clustering heatmap highlights the differential accumulation of fatty acid and associated pathway metabolites ($FC > 1$) that govern resistance. **(A)** Fatty acids involved in *B. tabaci*-tomato interaction. **(B)** Fatty acids involved in *P. absoluta*-tomato interaction. The heatmaps depict the clustering patterns of metabolites based on their abundance levels, providing insights into the metabolites activated during each interaction.

diagnose whitefly-infested tomatoes⁷⁷. Likewise, maize roots damaged by Asian cockchafer, *Holotrichia parallela* Motschulsky larvae exhibited elevated jasmonic acid and volatile production⁷⁸. In *Arabidopsis*, oviposition by the cabbage white butterfly, *Pieris brassicae* Linnaeus led to changes in tetracosanoic acid, attracting the egg parasitoid, *Trichogramma brassicae* Bezdenko⁷⁹.

Furthermore, pentacosane application in tomato enhanced egg parasitoid, *Trichogramma chilonis* Ishii efficacy against fruit borer, *H. armigera*⁸⁰, and pentacosane-treated *Coryca cephalonica* Stainton egg cards received the highest parasitism by *Trichogramma brasiliensis* Ashmead and *Trichogramma exiguum* Pinto & Platner⁸¹. Similarly, elevated levels of 2-heptanone and 2-heptanol following *N. lugens* infestation repelled further colonization of *N. lugens* while attracting natural enemies⁸². *M. destructor* enhanced palmitic acid levels in wheat and rice⁸³. Meanwhile, aphid, *Aphis glycines* Matsumura infestations enhance palmitic acid levels in soybeans⁸⁴. Similarly, *N. lugens* infestation in rice resulted in modified fatty acid concentrations, including triacontanoic and octadecadienoic acids, altered sugars and amino acids⁴⁴. Likewise, paddy swarming caterpillar, *Spodoptera mauritia* Boisduval infestation led to the accumulation of p-coumaroyl putrescine and feruloyl putrescine in rice⁸⁵, while rice striped stem borer, *Chilo suppressalis* Walker feeding increased tryptophan-derived, serotonin feruloyl tryptamine and p-coumaroyl serotonin in rice⁸⁶. Similarly, Dangol et al.⁸⁷ discovered elevated serotonin levels in green foxtail millet infested with aphid, *Rhopalosiphum padi* Linnaeus, which inhibited *R. padi*. In contrast, serotonin-deficient rice mutants resisted *N. lugens* and *C. suppressalis*⁸⁸.

Furthermore, elevated sebatic acid levels were observed in Vietnam robusta coffee seeds infected with coffee berry borer, *Hypothenemus hampei* Ferrari⁸⁹. Wheat aphid, *Schizaphis graminum* Rondani infestation in barley increased 1-octadecene levels, serving as a defense response⁹⁰. Zhang et al.⁹¹ found significant alterations in hexadecanoic, eicosanoic, docosanoic, and linoleic acid levels during *N. lugens* feeding in the resistant transgenic line (R6) and susceptible wild type (Nipponbare rice). Similarly, *Arabidopsis* plants, infested by *M. persicae*, exhibited elevated *TPS11* gene expression, which encodes trehalose-6-phosphate synthase/phosphatase for trehalose synthesis, regulating defense against *M. persicae*⁹². Likewise, *S. exigua* feeding in *Arabidopsis* induced ceramides, hydroxyceramide, and glucosylceramides, associated with jasmonate signaling³⁰. Similarly, hydroxyjasmonic acid was produced as a wound response in *Arabidopsis* leaves⁹³. Jasmonic acid derivative, hydroxyjasmonic acid accumulated in apple leaves during leaf miner, *Phyllonorycter blancardella* Fabricius infestation⁹⁴. Moreover, tomato plants treated with *Trichoderma* and infested by *M. euphorbiae* demonstrated increased levels of the stress-responsive signaling intermediate O-phosphoryl ethanolamine⁹⁵.

Fatty acids related to plant defense signaling

Cis-jasmone, derived from jasmonic acid, enhances plant resistance through up-regulation of octadecanoid biosynthesis genes⁹⁶. Hexadecatrienoic acid, derived from chloroplast lipids, serves as a precursor for jasmonic acid biosynthesis⁹⁷. In *Arabidopsis*, the hexadecanoid pathway, as a parallel route for JA biosynthesis, generates defense signaling molecules such as 2-oxo-phytodienoic acid (OPDA) and dinor-12-oxo-phytodienoic acid (dn-OPDA) through hexadecatrienoic acid (HTA)⁹⁸. Similarly, linoleic acid and linolenic acid served as lipoxygenase enzyme substrates, with linoleic acid metabolizing to 9,10-dihydro jasmonic acid as an alternate wound signal in bean, *Phaseolus vulgaris* Linnaeus⁹⁹. *Arabidopsis* mutant deficient in linolenic acid and linolenate displayed increased susceptibility to fungal gnat larvae, *Bradysia impatiens* Johannsen¹⁰⁰.

Furthermore, linolenic acid, derived from membrane lipids, transforms hydroperoxy linolenate by lipoxygenase (LOX), generating green leaf volatiles and jasmonic acid, activating genes for proteinase inhibitors and anti-herbivore factors¹⁰¹. Monogalactosyldiacylglycerols (MGDGs) play a crucial role in jasmonic acid biosynthesis; reduced MGDG synthesis in transgenic tobacco leads to lower jasmonic acid levels and increased vulnerability to *H. armigera*⁹⁷. Linolipin B and linolipin G are MGDGs and digalactosylmonoacylglycerol (DGDGs) and act as precursors for jasmonic acid synthesis⁹⁷. Sphinganine, a bioactive long chain base (LCB), serves as a precursor for other LCBs and plays a role in stress response. Overexpressing the *OsLCB2a1* gene in *A. thaliana* enhanced sphinganine, phytosphingosine, and phytoceramide levels, reducing *M. persicae* infestation^{102,103}. LCBs, including sphinganine and LCB2a gene, are implicated in programmed cell death, contributing to effective defense¹⁰⁴.

In this study, the abundance of fatty acid profiles is attributed to the fact that these profiles reflect both the types and quantities of specific fatty acids present in a genotype's acylsugars, a blend of acylsugars and sugar moiety²⁰. Notably, acylsugars in tomatoes constitute a vital category of defense metabolites^{105–107}. As a result, breeding tomato lines with varying levels of acylsugars or with distinct fatty acid profiles are beneficial^{108,109}. This metabolomics study represents well-characterized tomato parental material from which resistant populations can be developed. The information generated can be integrated into other functional genomics studies like transcriptomics, proteomics can provide a better understanding of the function of individual genes, as well as the crosstalk among genes, proteins and metabolites conferring resistance, which aid in developing resistant varieties^{110,111}. Future studies focusing on metabolic qualitative trait loci (mQTLs) and genome-wide association studies (mGWAS) can identify genotype–phenotype relationships, genetic variants linked to metabolic traits, and construct high-density maps of candidate genes^{112,113}. Moreover, metabolic engineering can be leveraged for selective breeding by modifying host plant genes, optimizing metabolic pathways for increased production of desired metabolites, and improving resistance to biotic stress^{114,115}. Therefore, understanding the gene regulatory mechanisms is required to utilize these advanced tools to effectively transfer resistance traits from wild species to cultivated tomatoes.

Materials and methods

Plant material and growth conditions

Three resistant wild tomato accessions (*S. cheesmaniae* VI037240-7 [V7], *S. galapagense* VI057400-3 [V3], and VI063177-10 [V10]) and two susceptible cultivated accessions (*S. lycopersicum* Hawaii-7996 [H6] and CLN-

5915 [C5] which we previously reported¹⁴ were grown in pots filled with a sterilized potting mixture (2:2:1 ratio of black soil, sand, and vermicompost) in a glasshouse ($27 \pm 1^\circ\text{C}$, $70 \pm 10\%$ RH, 12:12 light–dark cycles).

Rearing and maintenance of insects

The two insect species used in the study, *B. tabaci* and *P. absoluta*, were reared on eggplants and tomato plants, respectively, within a cage ($45 \times 45 \times 45$ cm) inside a glasshouse at ICRISAT, Hyderabad, India (17.5111°N , 78.2752°E) under controlled conditions ($27 \pm 1^\circ\text{C}$, $70 \pm 10\%$ RH, and 12:12 h light–dark cycle). Adult *B. tabaci* and second-instar larvae (green in color, 5–6 days old and around 2.6 mm in length) of *P. absoluta* were used for plant–herbivore interaction experiments.

Plant–herbivore interactions and sample collection

Plant–herbivore interactions and metabolomics were carried out on insect-infested (treated) and uninfested (control/mock) six-week-old plants from each accession (total five accessions) at two time points: 6- and 12-h post-infestation (hpi). This approach was used to capture early and late responses, allowing for the detection of temporal changes in metabolite expression following insect attack. Plant–herbivore interactions were conducted inside a glasshouse ($27 \pm 1^\circ\text{C}$, $70 \pm 10\%$ RH, and 12:12 h light–dark cycle), where the test insects, *B. tabaci* (ten adults) and *P. absoluta* (five second-instar larvae) were released into each clip cages (2.5 cm radius and 1.5 cm depth) installed on the second or third leaf of each accession and allowed to feed. In the corresponding mock plants, clip cages were installed similar to the treatment, but no insects were released. After each interaction (6 and 12 hpi separately for two insects), the clip cages were gently opened, and insects were removed from treated plants using forceps. In mock plants, the insect removal procedure was reproduced to balance the effect of forceps contact on possible induction of metabolic changes. Leaf samples were collected in a vial (Tarsons 15 mL graduated centrifuge tube), flash-frozen in liquid nitrogen and stored at -80°C . A separate set of interactions was performed for *B. tabaci* and *P. absoluta* at 6 and 12 hpi, with each accession (three resistant and two susceptible accessions) replicated thrice in both treated and mock conditions, resulting in 30 samples for each insect interaction at each time point and making a total of 120 samples: RP (resistant accession with pest infestation), RM (resistant accession with mock infestation), SP (susceptible accession with pest infestation), and SM (susceptible accession with mock infestation) (Fig. 1).

Metabolite extraction and LC-high-resolution MS (LC-HRMS) analysis

A 100 mg leaf sample was homogenized into a fine powder¹¹⁶. The metabolites were then extracted using 80% aqueous methanol with 0.1% formic acid¹¹⁷. The extracted metabolites were analyzed in a positive ionization mode using The Waters I-Class Ultra Performance Liquid Chromatography coupled to a Waters Xevo G2-XS utilizing Electrospray Ionization-Quadrupole Time of Flight-Mass Spectrometry system (UPLC-XEVO-G2-XS-ESI-QTOF) equipped with an ACQUITY C18 column (10 cm \times 2.1 mm, particle size 1.7 μm , Waters) containing LC–MS grade water in 0.1% formic acid (v/v; mobile phase A) and methanol in 0.1% formic acid (mobile phase B). The mass resolution was set from m/z 50 to 2000 and was recorded in centroid mode. Standard mass calibration was achieved using leucine enkephalin (Leu-Enk, m/z 554.262), and MS/MS fragmentations were performed at a normalized collision energy of 40 eV. Data was collected using MassLynx™ V4.1 workstation in continuum mode¹¹⁸.

LC-HRMS data processing

The LC-HRMS output raw data files were converted into mzXML format using MZmine-2 with the high-sensitivity peak detection algorithm ADAP wavelets¹¹⁹. Subsequently, the observed masses, m/z values, retention time, and abundance (relative intensity) of compounds were imported to MS Excel. Peaks exhibiting inconsistency across replicates and those annotated as isotopes and adducts were omitted from further analysis.

Metabolomic data analysis

Peak height data of compounds were exported and formatted for data analysis. Metabolites were putatively identified based on two criteria: (1) accurate mass match (accurate mass error (AME) < 5 ppm) with metabolites reported in different databases such as METLIN, Plant Metabolic Network (PMN), LIPID MAPS, and KEGG, and (2) fragmentation pattern match with those in databases or in silico verification¹²⁰. The data with the abundance of metabolites in samples (RM, RP, SM, and SP) with three biological replicates were averaged and subjected to pairwise Student's *t*-test for four comparisons: RM_ SM, RP_SP, RP_RM, and SP_ SM. The fold change (FC) difference was calculated as the average concentration of metabolites in resistant samples to that in susceptible samples. Differentially accumulated metabolites were selected using the criteria of $P < 0.05$ and $\log_2\text{FC} > 1.0$. RR metabolites are those that show a higher abundance in resistant samples than in susceptible ones. So, six combinations of resistant vs. susceptible accessions (R vs. S) were made: V3 vs. C5, V3 vs. H6, V7 vs. C5, V7 vs. H6, V10 vs. C5 and V10 vs. H6, to identify RR metabolites along with FC difference and cumulative difference in FC was also calculated.

These RR metabolites were further grouped into resistance-related constitutive (RRC) and induced (RRI) metabolites using the following formulas, $\text{RRC} = \text{RM}/\text{SM}$ and $\text{RRI} = (\text{RP}/\text{RM})/(\text{SP}/\text{SM})$, where RP (resistant accession with pest infestation), RM (resistant accession with mock infestation), SP (susceptible accession with pest infestation), and SM (susceptible accession with mock infestation)¹²⁰. The multivariate, Partial least squares-discriminant analysis (PLS-DA) was performed using peak height data to determine the differences in metabolic profiles of treated and mock samples between resistant and susceptible tomato accessions. Similarly, volcano plot analysis was performed to determine the upregulated and downregulated metabolites in treated and mock samples of tomato accessions. Additionally, hierarchical clustering heat maps were used to visualize the differential accumulation of metabolites in R vs. S comparisons using MetaboAnalyst 5.0 (<https://www.me>

taboanalyst.ca). Furthermore, Venn diagrams were generated to determine the unique and shared metabolites using Venny 2.1 (<https://bioinfogp.cnb.csic.es/tools/venny/>). An overview of metabolomics experimental setup and data analysis is illustrated in Fig. 1.

Conclusion

Understanding the resistance mechanisms in wild tomato accessions is crucial for breeding initiatives. Our non-targeted metabolomics approach successfully identified key metabolic responses in resistant wild and susceptible cultivated tomato accessions to herbivory by *B. tabaci* Asia II 7 and *P. absoluta*. We observed differences in metabolic profiles before and after infestation at 6 and 12 hpi uncovering several RR metabolites, particularly in the fatty acid and associated biosynthesis pathways, which are involved in the plant defense mechanisms. These metabolites, spanning multiple chemical groups, exhibit various roles in insect deterrence, plant–insect interactions and plant defense signaling. Our findings offer valuable insights into the potential use of RR metabolites to enhance tomato resistance, contributing to more resilient crops with improved yield under biotic stress.

Data availability

The original contributions presented in the study are included in the article/supplementary material. Further inquiries can be directed to the corresponding author.

Received: 17 October 2024; Accepted: 8 January 2025

Published online: 30 January 2025

References

- Andrade, M. C. et al. Inheritance of type IV glandular trichome density and its association with whitefly resistance from *Solanum galapagense* accession LA1401. *Euphytica* **213**, 52 (2017).
- Czosnek, H. & Laterrot, H. A worldwide survey of tomato yellow leaf curl viruses. *Arch. Virol.* **142**, 1391–1406 (1997).
- Kanakala, S. & Ghanim, M. Global genetic diversity and geographical distribution of *Bemisia tabaci* and its bacterial endosymbionts. *PLOS ONE* **14**, e0213946 (2019).
- Dias, D. M. et al. Resistance of processing tomato genotypes to leafminer (*Tuta absoluta*). *Hortic. Bras.* **37**, 40–46 (2019).
- Guedes, R. N. C. et al. Insecticide resistance in the tomato pinworm *Tuta absoluta*: patterns, spread, mechanisms, management and outlook. *J. Pest Sci.* **92**, 1329–1342 (2019).
- Horowitz, A. R., Ghanim, M., Roditakis, E., Nauen, R. & Ishaaya, I. Insecticide resistance and its management in *Bemisia tabaci* species. *J. Pest Sci.* **93**, 893–910 (2020).
- Mithöfer, A. & Boland, W. Plant defense against herbivores: chemical aspects. *Annu. Rev. Plant Biol.* **63**, 431–450 (2012).
- Kersch-Becker, M. F., Thaler, J. S. & Mónica Kersch-Becker, C. F. Constitutive and herbivore-induced plant defences regulate herbivore population processes. *J. Anim. Ecol.* **88**, 1079–1088 (2019).
- Jiang, Y., Zhang, C. X., Chen, R. & He, S. Y. Challenging battles of plants with phloem-feeding insects and prokaryotic pathogens. *Proc. Natl. Acad. Sci. U. S. A.* **116**, 23390–23397 (2019).
- Kortbeek, R. W. J. et al. Natural variation in wild tomato trichomes; selecting metabolites that contribute to insect resistance using a random forest approach. *BMC Plant Biol.* **21**, 315 (2021).
- Rakha, M., Hanson, P. & Ramasamy, S. Identification of resistance to *Bemisia tabaci* Genn. in closely related wild relatives of cultivated tomato based on trichome type analysis and choice and no-choice assays. *Genet. Resour. Crop Evol.* **64**, 247–260 (2017).
- Ghosh, P. et al. Performance of Wild Tomato Accessions and Elucidation of Resistance against Invasive Pest *Phthorimaea absoluta* Damage under Tropical Conditions. *Horticulturae* **9**, 143–143 (2023).
- Mahmoud, A. M. A. et al. *Tuta absoluta* (Meyrick) resistance in tomato (*Solanum lycopersicum* L.) accessions and species. <https://doi.org/10.1080/09670874.2022.2055195> 1–13 (2022) <https://doi.org/10.1080/09670874.2022.2055195>.
- Kumaraswamy, S., Sotelo-Cardona, P., Shivanna, A., Mohan, M. & Srinivasan, R. Evaluation of resistance in wild tomato accessions to the whitefly *Bemisia tabaci* and the invasive tomato leafminer *Tuta absoluta*. *Entomol. Gen.* <https://doi.org/10.1127/entomologia/2024/2368> (2024).
- Su, Q. et al. Whitefly aggregation on tomato is mediated by feeding-induced changes in plant metabolites that influence the behaviour and performance of conspecifics. *Funct. Ecol.* **32**, 1180–1193 (2018).
- Sade, D. et al. Comparative metabolomics and transcriptomics of plant response to Tomato yellow leaf curl virus infection in resistant and susceptible tomato cultivars. *Metabolomics* **11**, 81–97 (2015).
- Rossouw, L. T. et al. Deciphering the resistance mechanism of tomato plants against whitefly-mediated tomato curly stunt virus infection through ultra-high-performance liquid chromatography coupled to mass spectrometry (Uhp-lc-ms)-based metabolomics approaches. *Metabolites* **9**, (2019).
- Roumani, M. et al. Transcriptomics and Metabolomics Analyses Reveal High Induction of the Phenolamide Pathway in Tomato Plants Attacked by the Leafminer *Tuta absoluta*. *Metabolites* **12**, 484 (2022).
- de Falco, B. et al. Metabolomics approach based on NMR spectroscopy and multivariate data analysis to explore the interaction between the leafminer *Tuta absoluta* and tomato (*Solanum lycopersicum*). *Phytochem. Anal. PCA* **30**, 556–563 (2019).
- Ben-Mahmoud, S. et al. Acylsugar amount and fatty acid profile differentially suppress oviposition by western flower thrips, *Frankliniella occidentalis*, on tomato and interspecific hybrid flowers. *PLoS ONE* **13**, (2018).
- Kant, M. R., Ament, K., Sabelis, M. W., Haring, M. A. & Schuurink, R. C. Differential Timing of Spider Mite-Induced Direct and Indirect Defenses in Tomato Plants. *Plant Physiol.* **135**, 483–495 (2004).
- Allwood, J. W. et al. Unravelling Plant Responses to Stress—The Importance of Targeted and Untargeted Metabolomics. *Metabolites* **11**, 558 (2021).
- Anzano, A., Bonanomi, G., Mazzoleni, S. & Lanzotti, V. Plant metabolomics in biotic and abiotic stress: a critical overview. *Phytochem. Rev.* **21**, 503–524 (2022).
- Piasecka, A., Kachlicki, P. & Stobiecki, M. Analytical Methods for Detection of Plant Metabolomes Changes in Response to Biotic and Abiotic Stresses. *Int. J. Mol. Sci.* **20**, 379 (2019).
- Rosato, A. et al. From correlation to causation: analysis of metabolomics data using systems biology approaches. *Metabolomics* **14**, 37 (2018).
- Villate, A. et al. Review: Metabolomics as a prediction tool for plants performance under environmental stress. *Plant Sci.* **303**, 110789 (2021).
- Stam, J. M. et al. Plant interactions with multiple insect herbivores: from community to genes. *Annu. Rev. Plant Biol.* **65**, 689–713 (2014).

28. Sanchez-Arcos, C., Reichelt, M., Gershenson, J. & Kunert, G. Modulation of Legume Defense Signaling Pathways by Native and Non-native Pea Aphid Clones. *Front. Plant Sci.* **7**, 1872 (2016).
29. Ali, J. G. & Agrawal, A. A. Specialist versus generalist insect herbivores and plant defense. *Trends Plant Sci.* **17**, 293–302 (2012).
30. Huang, L.-Q. et al. Arabidopsis alkaline ceramidase ACER functions in defense against insect herbivory. *J. Exp. Bot.* **73**, 4954–4967 (2022).
31. War, A. R. et al. Mechanisms of plant defense against insect herbivores. *Plant Signal. Behav.* **7**, 1306–1320 (2012).
32. Errard, A. et al. Single- versus Multiple-Pest Infestation Affects Differently the Biochemistry of Tomato (*Solanum lycopersicum* 'Ailsa Craig'). *J. Agric. Food Chem.* **63**, 10103–10111 (2015).
33. Steinbrenner, A. D., Gómez, S., Osorio, S., Fernie, A. R. & Orians, C. M. Herbivore-induced changes in tomato (*Solanum lycopersicum*) primary metabolism: a whole plant perspective. *J. Chem. Ecol.* **37**, 1294–1303 (2011).
34. Rodriguez-Saona, C., Chalmers, J. A., Raj, S. & Thaler, J. S. Induced plant responses to multiple damagers: differential effects on an herbivore and its parasitoid. *Oecologia* **143**, 566–577 (2005).
35. Rodriguez-Saona, C. R., Musser, R. O., Vogel, H., Hum-Musser, S. M. & Thaler, J. S. Molecular, Biochemical, and Organismal Analyses of Tomato Plants Simultaneously Attacked by Herbivores from Two Feeding Guilds. *J. Chem. Ecol.* **36**, 1043–1057 (2010).
36. Davidson-Lowe, E. & Ali, J. G. Herbivore-induced plant volatiles mediate behavioral interactions between a leaf-chewing and a phloem-feeding herbivore. *Basic Appl. Ecol.* **53**, 39–48 (2021).
37. Xue, M., Wang, C.-X., Bi, M.-J., Li, Q.-L. & Liu, T.-X. Induced Defense by *Bemisia tabaci* Biotype B (Hemiptera: Aleyrodidae) in Tobacco Against *Myzus persicae* (Hemiptera: Aphididae). *Environ. Entomol.* **39**, 883–891 (2010).
38. Kroes, A. et al. Plant-mediated interactions between two herbivores differentially affect a subsequently arriving third herbivore in populations of wild cabbage. *Plant Biol. Stuttg. Ger.* **18**, 981–991 (2016).
39. Eisenring, M., Glauser, G., Meissle, M. & Romeis, J. Differential Impact of Herbivores from Three Feeding Guilds on Systemic Secondary Metabolite Induction, Phytohormone Levels and Plant-Mediated Herbivore Interactions. *J. Chem. Ecol.* **44**, 1178–1189 (2018).
40. Karssemeijer, P. N., Reichelt, M., Gershenson, J., van Loon, J. & Dicke, M. Foliar herbivory by caterpillars and aphids differentially affects phytohormonal signalling in roots and plant defence to a root herbivore. *Plant Cell Environ.* **43**, 775–786 (2020).
41. Mewis, I. et al. Gene expression and glucosinolate accumulation in Arabidopsis thaliana in response to generalist and specialist herbivores of different feeding guilds and the role of defense signaling pathways. *Phytochemistry* **67**, 2450–2462 (2006).
42. Shrestha, K. et al. Disruption of the sorghum circadian clock impacts sorghum-sugarcane aphid interaction dynamics and aphid feeding behavior. *Plant Stress* **11**, 100407 (2024).
43. Uawisetwathana, U. et al. Global metabolite profiles of rice brown planthopper-resistant traits reveal potential secondary metabolites for both constitutive and inducible defenses. *Metabolomics Off. J. Metabolomic Soc.* **15**, 151 (2019).
44. Kang, K., Yue, L., Xia, X., Liu, K. & Zhang, W. Comparative metabolomics analysis of different resistant rice varieties in response to the brown planthopper *Nilaparvata lugens* Hemiptera: Delphacidae. *Metabolomics Off. J. Metabolomic Soc.* **15**, 62 (2019).
45. Firdaus, S. et al. Identification and QTL mapping of whitefly resistance components in *Solanum galapagense*. *Theor. Appl. Genet.* **126**, 1487–1501 (2013).
46. Yao, Q. et al. Tomato Plant Flavonoids Increase Whitefly Resistance and Reduce Spread of Tomato yellow leaf curl virus. *J. Econ. Entomol.* **112**, 2790–2796 (2019).
47. Yang, F. et al. Flavonoid production in tomato mediates both direct and indirect plant defences against whiteflies in tritrophic interactions. *Pest Manag. Sci.* **79**, 4644–4654 (2023).
48. Chen, L. et al. Comprehensive Metabolome and Volatilome Analyses in Eggplant and Tomato Reveal Their Differential Responses to *Tuta absoluta* Infestation. *Front. Plant Sci.* **12**, 2231–2231 (2021).
49. Germinara, G. S., Rotundo, G. & De Cristofaro, A. Repellence and fumigant toxicity of propionic acid against adults of *Sitophilus granarius* (L.) and *S. oryzae* (L.). *J. Stored Prod. Res.* **43**, 229–233 (2007).
50. Germinara, G. S. et al. Controlled Release of Propionic Acid and (E)-2-Hexenal Against *Sitophilus Granarius* (L.) (Coleoptera: Curculionidae). *J. Food Process. Preserv.* **39**, 123–130 (2015).
51. Cruz-Estrada, A. et al. Medium-Chain Fatty Acids from *Eugenia winzerlingii* Leaves Causing Insect Settling Deterrent, Nematicidal, and Phytotoxic Effects. *Molecules* **24**, 1724 (2019).
52. Jiang, H. et al. Chemical composition of an insecticidal extract from *Robinia pseudacacia* L. seeds and its efficacy against aphids in oilseed rape. *Crop Prot.* **104**, 1–6 (2018).
53. Reddy, M. S. S., Agnihotri, M., Divija, S. D., Belal, B. & Karthik, S. Host plant resistance profiling of chickpea genotypes against *Helicoverpa armigera* (Hübner) through SEM and GC-MS studies. *Int. J. Trop. Insect Sci.* **42**, 1627–1638 (2022).
54. Dang, Q. L. et al. Insecticidal activities of crude extracts and phospholipids from *Chenopodium ficifolium* against melon and cotton aphid. *Aphis gossypii*. *Crop Prot.* **29**, 1124–1129 (2010).
55. Khajuria, C. et al. Mobilization of lipids and fortification of cell wall and cuticle are important in host defense against Hessian fly. *BMC Genomics* **14**, 423 (2013).
56. Eigenbrode, S. D., Espelie, K. E. & Shelton, A. M. Behavior of neonate diamondback moth larvae [*Plutella xylostella* (L.)] on leaves and on extracted leaf waxes of resistant and susceptible cabbages. *J. Chem. Ecol.* **17**, 1691–1704 (1991).
57. Yele, Y., Dhillon, M. K., Tanwar, A. K. & Kumar, S. Amino and fatty acids contributing to antibiosis against *Chilo partellus* (Swinhoe) in maize. *Arthropod-Plant Interact.* **15**, 721–736 (2021).
58. Pavunraj, M. et al. Silver nanoparticles containing stearic acid isolated from *Catharanthus roseus*: Ovicidal and oviposition-deterrent activities on *Earias vittella* and ecotoxicological studies. *Pestic. Biochem. Physiol.* **168**, 104640 (2020).
59. Oliveira, F. A., da Silva, D. J. H., Leite, G. L. D., Jham, G. N. & Picanço, M. Resistance of 57 greenhouse-grown accessions of *Lycopersicon esculentum* and three cultivars to *Tuta absoluta* (Meyrick) (Lepidoptera: Gelechiidae). *Sci. Hortic.* **119**, 182–187 (2009).
60. Cespedes, C. L. et al. The insecticidal, molting disruption and insect growth inhibitory activity of extracts from *Condalia microphylla* Cav. (Rhamnaceae). *Ind. Crops Prod.* **42**, 78–86 (2013).
61. Goffreda, J. C., Mutschler, M. A., Avé, D. A., Tingey, W. M. & Steffens, J. C. Aphid deterrence by glucose esters in glandular trichome exudate of the wild tomato. *Lycopersicon pennellii*. *J. Chem. Ecol.* **15**, 2135–2147 (1989).
62. Neal, J. J., Tingey, W. M. & Steffens, J. C. Sucrose esters of carboxylic acids in glandular trichomes of *Solanum berthaultii* deter settling and probing by green peach aphid. *J. Chem. Ecol.* **16**, 487–497 (1990).
63. Walters, D. S. & Steffens, J. C. Branched Chain Amino Acid Metabolism in the Biosynthesis of *Lycopersicon pennellii* Glucose Esters I. *Plant Physiol.* **93**, 1544–1551 (1990).
64. Chortyk, O. T., Pomonis, J. G. & Johnson, A. W. Syntheses and Characterizations of Insecticidal Sucrose Esters. *J. Agric. Food Chem.* **44**, 1551–1557 (1996).
65. McKenzie, C. L. & Puterka, G. J. Effect of Sucrose Octanoate on Survival of Nymphal and Adult *Diaphorina citri* (Homoptera: Psyllidae). *J. Econ. Entomol.* **97**, 970–975 (2004).
66. Bruce, T. J. A. et al. cis-Jasmone treatment induces resistance in wheat plants against the grain aphid, *Sitobion avenae* (Fabricius) (Homoptera: Aphididae). *Pest Manag. Sci.* **59**, 1031–1036 (2003).
67. Sobhy, I. S., Caulfield, J. C., Pickett, J. A. & Birkett, M. A. Sensing the Danger Signals: cis-Jasmone Reduces Aphid Performance on Potato and Modulates the Magnitude of Released Volatiles. *Front. Ecol. Evol.* **7**, (2020).

68. Sun, Y.-L. et al. An odorant receptor mediates the attractiveness of cis-jasmone to *Camponotus chloridiae*, the endoparasitoid of *Helicoverpa armigera*. *Insect Mol. Biol.* **28**, 23–34 (2019).
69. da Graça, J. P. et al. The natural plant stress elicitor cis-jasmone causes cultivar-dependent reduction in growth of the stink bug, *Euschistus heros* and associated changes in flavonoid concentrations in soybean. *Glycine max. Phytochemistry* **131**, 84–91 (2016).
70. Paprocka, M., Gliszczyska, A., Danciewicz, K. & Gabryś, B. Novel Hydroxy- and Epoxy-cis-Jasmone and Dihydrojasmone Derivatives Affect the Foraging Activity of the Peach Potato Aphid *Myzus persicae* (Sulzer) (Homoptera: Aphididae). *Mol. Basel Switz.* **23**, 2362 (2018).
71. Birkett, M. A. et al. New roles for cis-jasmone as an insect semiochemical and in plant defense. *Proc. Natl. Acad. Sci.* **97**, 9329–9334 (2000).
72. Savchenko, T. et al. Arachidonic Acid: An Evolutionarily Conserved Signaling Molecule Modulates Plant Stress Signaling Networks[C][W]. *Plant Cell* **22**, 3193–3205 (2010).
73. Rivard, D., Cloutier, C. & Michaud, D. Colorado potato beetles show differential digestive compensatory responses to host plants expressing distinct sets of defense proteins. *Arch. Insect Biochem. Physiol.* **55**, 114–123 (2004).
74. Colazza, S., McElfresh, J. S. & Millar, J. G. Identification of Volatile Synomones, Induced by *Nezara viridula* Feeding and Oviposition on Bean spp., That Attract the Egg Parasitoid *Trissolcus basalis*. *J. Chem. Ecol.* **30**, 945–964 (2004).
75. Farag, M. A. & Paré, P. W. C6-Green leaf volatiles trigger local and systemic VOC emissions in tomato. *Phytochemistry* **61**, 545–554 (2002).
76. Paré, P. W. & Tumlinson, J. H. Plant Volatiles as a Defense against Insect Herbivores. *Plant Physiol.* **121**, 325–332 (1999).
77. Cui, S., Cao, L., Acosta, N., Zhu, H. & Ling, P. P. Development of Portable E-Nose System for Fast Diagnosis of Whitefly Infestation in Tomato Plant in Greenhouse. *Chemosensors* **9**, 297 (2021).
78. Pan, Y. et al. The herbivore-induced plant volatile tetradecane enhances plant resistance to *Holotrichia parallela* larvae in maize roots. *Pest Manag. Sci.* **78**, 550–560 (2022).
79. Blenn, B. et al. Insect egg deposition induces indirect defense and epicuticular wax changes in *Arabidopsis thaliana*. *J. Chem. Ecol.* **38**, 882–892 (2012).
80. Paul, A. V. N., Srivastava, M., Dureja, P. & Singh, A. K. Semiochemicals produced by tomato varieties and their role in parasitism of *Corycra cephalonica* (Lepidoptera: Pyralidae) by the egg parasitoid *Trichogramma chilonis* (Hymenoptera: Trichogrammatidae). *Int. J. Trop. Insect Sci.* **28**, 108–116 (2008).
81. Paul, A. V. N., Singh, S. & Singh, A. K. Kairomonal effect of some saturated hydrocarbons on the egg parasitoids, *Trichogramma brasiliensis* (Ashmead) and *Trichogramma exiguum*, Pinto, Platner and Oatman (Hym., Trichogrammatidae). *J. Appl. Entomol.* **126**, 409–416 (2002).
82. Lu, J. et al. Contrasting effects of ethylene biosynthesis on induced plant resistance against a chewing and a piercing-sucking herbivore in rice. *Mol. Plant* **7**, 1670–1682 (2014).
83. Zhu, L., Chen, M.-S. & Liu, X. Changes in phytohormones and fatty acids in wheat and rice seedlings in response to Hessian fly (Diptera: Cecidomyiidae) infestation. *J. Econ. Entomol.* **104**, 1384–1392 (2011).
84. Kanobe, C., McCarville, M. T., O’Neal, M. E., Tylka, G. L. & MacIntosh, G. C. Soybean Aphid Infestation Induces Changes in Fatty Acid Metabolism in Soybean. *PLOS ONE* **10**, e0145660 (2015).
85. Tanabe, K., Hojo, Y., Shinya, T. & Galis, I. Molecular evidence for biochemical diversification of phenolamide biosynthesis in rice plants. *J. Integr. Plant Biol.* **58**, 903–913 (2016).
86. Ishihara, A., Hashimoto, Y., Miyagawa, H. & Wakasa, K. Induction of serotonin accumulation by feeding of rice striped stem borer in rice leaves. *Plant Signal. Behav.* **3**, 714–716 (2008).
87. Dangol, A., Yaakov, B., Jander, G., Strickler, S. R. & Tzin, V. Characterizing the serotonin biosynthesis pathway upon aphid infestation in *Setaria viridis* leaves. 642041 Preprint at <https://doi.org/10.1101/642041> (2019).
88. Lu, H.-P. et al. Resistance of rice to insect pests mediated by suppression of serotonin biosynthesis. *Nat. Plants* **4**, 338–344 (2018).
89. Castro-Moretti, F. R., Cocuron, J.-C., Vega, F. E. & Alonso, A. P. Differential Metabolic Responses Caused by the Most Important Insect Pest of Coffee Worldwide, the Coffee Berry Borer (*Hypothenemus hampei*). *J. Agric. Food Chem.* **68**, 2597–2605 (2020).
90. Muñoz, O., Argandoña, V. H. & Corcuera, L. J. Chemical Constituents from Shoots of *Hordeum vulgare* Infested by the Aphid *Schizaphis graminum*. *Z. Für Naturforschung C* **53**, 811–817 (1998).
91. Zhang, J. et al. Lipid profiles reveal different responses to brown planthopper infestation for pest susceptible and resistant rice plants. *Metabolomics Off. J. Metabolomic Soc.* **14**, 120 (2018).
92. Singh, V. et al. TREHALOSE PHOSPHATE SYNTHASE11-dependent trehalose metabolism promotes *Arabidopsis thaliana* defense against the phloem-feeding insect *Myzus persicae*. *Plant J. Cell Mol. Biol.* **67**, 94–104 (2011).
93. Widemann, E. et al. The amidohydrolases IAR3 and ILL6 contribute to jasmonoyl-isoleucine hormone turnover and generate 12-hydroxyjasmonic acid upon wounding in *Arabidopsis* leaves. *J. Biol. Chem.* **288**, 31701–31714 (2013).
94. Zhang, H. et al. Leaf-mining by *Phyllonorycter blancardella* reprograms the host-leaf transcriptome to modulate phytohormones associated with nutrient mobilization and plant defense. *J. Insect Physiol.* **84**, 114–127 (2016).
95. Coppola, M. et al. Transcriptome and Metabolome Reprogramming in Tomato Plants by *Trichoderma harzianum* strain T22 Primes and Enhances Defense Responses Against Aphids. *Front. Physiol.* **10**, 745 (2019).
96. Matthes, M. C. et al. The transcriptome of cis-jasmone-induced resistance in *Arabidopsis thaliana* and its role in indirect defence. *Planta* **232**, 1163–1180 (2010).
97. Wang, J. Monogalactosyldiacylglycerol deficiency affects jasmonic acid biosynthesis and defense responses to insect herbivores in *Nicotiana glauca*. *Plant Sci.* **176**, 279–285 (2009).
98. Weber, H., Vick, B. A. & Farmer, E. E. Dinor-oxo-phytyldienoic acid: A new hexadecanoid signal in the jasmonate family. *Proc. Natl. Acad. Sci. U. S. A.* **94**, 10473–10478 (1997).
99. Blechert, S. et al. The octadecanoic pathway: Signal molecules for the regulation of secondary pathways. *Proc. Natl. Acad. Sci. U. S. A.* **92**, 4099–4105 (1995).
100. McConn, M., Creelman, R. A., Bell, E., Mullet, J. E. & Browse, J. Jasmonate is essential for insect defense in *Arabidopsis*. *Proc. Natl. Acad. Sci. U. S. A.* **94**, 5473–5477 (1997).
101. Turner, J. G., Ellis, C. & Devoto, A. The jasmonate signal pathway. *Plant Cell* **14**, s153–s164 (2002).
102. Begum, M. A. et al. Molecular Characterization of Rice OsLCB2a1 Gene and Functional Analysis of its Role in Insect Resistance. *Front. Plant Sci.* **7**, (2016).
103. Chen, M., Han, G., Dietrich, C. R., Dunn, T. M. & Cahoon, E. B. The essential nature of sphingolipids in plants as revealed by the functional identification and characterization of the *Arabidopsis* LCB1 subunit of serine palmitoyltransferase. *Plant Cell* **18**, 3576–3593 (2006).
104. Saucedo-García, M. et al. MPK6, sphinganine and the LCB2a gene from serine palmitoyltransferase are required in the signaling pathway that mediates cell death induced by long chain bases in *Arabidopsis*. *New Phytol.* **191**, 943–957 (2011).
105. Glas, J. J. et al. Plant glandular trichomes as targets for breeding or engineering of resistance to herbivores. *Int. J. Mol. Sci.* **13**, 17077–17103 (2012).
106. Lucatti, A. F., Van Heusden, A. W., Ch De Vos, R., Gf Visser, R. & Vosman, B. Differences in Insect Resistance between Tomato Species Endemic to the Galapagos Islands. <http://www.biomedcentral.com/1471-2148/13/175> (2013).
107. Vosman, B. et al. Broad spectrum insect resistance and metabolites in close relatives of the cultivated tomato. *Euphytica* **214**, 46 (2018).

108. Leckie, B. M., De Jong, D. M. & Mutschler, M. A. Quantitative trait loci increasing acylsugars in tomato breeding lines and their impacts on silverleaf whiteflies. *Mol. Breed.* **30**, 1621–1634 (2012).
109. Smeda, J. R., Schillmiller, A. L., Last, R. L. & Mutschler, M. A. Introgression of acylsugar chemistry QTL modifies the composition and structure of acylsugars produced by high-accumulating tomato lines. *Mol. Breed.* **36**, 160 (2016).
110. Buell, C. R. & Voytas, D. Technology Turbocharges Functional Genomics. *Plant Cell* **29**, 1179–1180 (2017).
111. Perez-Fons, L. et al. A metabolomics characterisation of natural variation in the resistance of cassava to whitefly. *BMC Plant Biol.* **19**, 518 (2019).
112. Fang, C. & Luo, J. Metabolic GWAS-based dissection of genetic bases underlying the diversity of plant metabolism. *Plant J.* **97**, 91–100 (2019).
113. Fernandez, O. et al. Fortune telling: metabolic markers of plant performance. *Metabolomics* **12**, 158 (2016).
114. Tatsis, E. C. & O'Connor, S. E. New developments in engineering plant metabolic pathways. *Curr. Opin. Biotechnol.* **42**, 126–132 (2016).
115. Yang, C. et al. A regulatory gene induces trichome formation and embryo lethality in tomato. *Proc. Natl. Acad. Sci. U. S. A.* **108**, 11836–11841 (2011).
116. Salem, M., Bernach, M., Bajdzienko, K. & Gialvalisco, P. A Simple Fractionated Extraction Method for the Comprehensive Analysis of Metabolites, Lipids, and Proteins from a Single Sample. *J. Vis. Exp. JoVE* 55802. <https://doi.org/10.3791/55802> (2017).
117. De Vos, R. C. H. et al. Untargeted large-scale plant metabolomics using liquid chromatography coupled to mass spectrometry. *Nat. Protoc.* **2**, 778–791 (2007).
118. Avuthu, T. et al. Comparative metabolomics analysis reveals secondary cell wall thickening as a barrier to resist *Aspergillus flavus* infection in groundnut. *Physiol. Plant.* **176**, e14169 (2024).
119. Pluskal, T., Castillo, S., Villar-Briones, A. & Orešič, M. MZmine 2: Modular framework for processing, visualizing, and analyzing mass spectrometry-based molecular profile data. *BMC Bioinf.* **11**, 395 (2010).
120. Yogendra, K. N. et al. Transcription factor StWRKY1 regulates phenylpropanoid metabolites conferring late blight resistance in potato. *J. Exp. Bot.* **66**, 7377–7389 (2015).

Acknowledgements

We sincerely thank the World Vegetable Center-South and Central Asia Regional Office and ICRISAT for the research facilities.

Author contributions

Conceptualization, S.K., K.Y., P.S.-C., and R.S.; Formal analysis, S.K., K.Y., A.S., and S.H.; Funding acquisition, R.S.; Investigation, S.K.; Methodology, S.K., K.Y., P.S.-C., A.S., and R.S.; Project administration, P.S.-C., and R.S.; Supervision, K.Y., P.S.-C., A.S., M.M. and R.S.; Writing-original draft, S.K.; Writing-review & editing, K.Y., P.S.-C., A.S., M.M. and R.S. All authors have read and agreed to the published version of the manuscript.

Funding

This study was funded by the World Vegetable Center, Taiwan, under the Student Research Fellowship Program 2021–2022, and by long-term strategic donors to the World Vegetable Center: Taiwan, the Foreign, the Commonwealth & Development Office (FCDO) from the UK government, United States Agency for International Development (USAID), Australian Centre for International Agricultural Research (ACIAR), Germany, Thailand, Philippines, Korea, and Japan.

Declarations

Competing interests

The authors declare no competing interests.

Ethics statement

This research did not involve animals. However, all the experimental procedures involving insects were conducted with care, and efforts were made to minimize harm to the insects throughout the study.

Additional information

Supplementary Information The online version contains supplementary material available at <https://doi.org/10.1038/s41598-025-86191-9>.

Correspondence and requests for materials should be addressed to R.S.

Reprints and permissions information is available at www.nature.com/reprints.

Publisher's note Springer Nature remains neutral with regard to jurisdictional claims in published maps and institutional affiliations.

Open Access This article is licensed under a Creative Commons Attribution-NonCommercial-NoDerivatives 4.0 International License, which permits any non-commercial use, sharing, distribution and reproduction in any medium or format, as long as you give appropriate credit to the original author(s) and the source, provide a link to the Creative Commons licence, and indicate if you modified the licensed material. You do not have permission under this licence to share adapted material derived from this article or parts of it. The images or other third party material in this article are included in the article's Creative Commons licence, unless indicated otherwise in a credit line to the material. If material is not included in the article's Creative Commons licence and your intended use is not permitted by statutory regulation or exceeds the permitted use, you will need to obtain permission directly from the copyright holder. To view a copy of this licence, visit <http://creativecommons.org/licenses/by-nc-nd/4.0/>.

© The Author(s) 2025